

119
85

IMPACT RESPONSE OF INTERLEAVED COMPOSITE MATERIALS

by

Gajanan V Gandhe

thesis submitted to the Faculty of the

Virginia Polytechnic Institute and State University

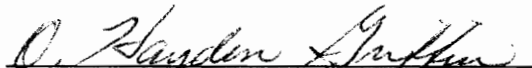
in partial fulfillment of the requirements for the degree of

Master of Science

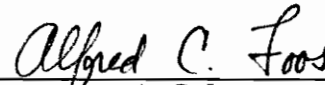
in

Engineering Mechanics

APPROVED:


O. Hayden Griffin, Chairperson


E. G. Henneke


A. C. Loos

December 1988

Blacksburg, Virginia

,2

LD
5655
V855
1988
G353
C.2

IMPACT RESPONSE OF INTERLEAVED COMPOSITE MATERIALS

by

Gajanan V Gandhe

O. Hayden Griffin, Chairperson

Engineering Mechanics

(ABSTRACT)

12/11/17
202

The need for better impact resistant composites has resulted in the development of many toughened resin systems. A combination of a tougher resin system along with higher strength fibers increases the impact resistance of the composite. The use of an adhesive layer between two plies of the improved prepreg system has been found to considerably increase the impact resistance. This concept is known as 'Interleafing'.

This investigation studies the response of the interleaf materials to instrumented drop weight impact as compared with the response of non-interleaved materials. Two non-destructive quality evaluation techniques, namely, ultrasonics and eddy currents, are used to qualitatively evaluate the damage developed in the specimens. Several different energy levels of damage are studied.

The interleaved laminate had significantly better impact response than the non-interleaved laminate for the same impact energy. The onset of delamination was delayed by the use of the interleaf. Whereas damage could be detected at an impact energy as low as 1.75 ft-lb in the baseline laminate; the interleaved laminate did not show any ultrasonic C-scan indication upto an impact of 2.45 ft-lb. The increase of delamination with increasing impact energy was slower in the interleaved specimen.

The eddy current method is not effective in detecting damage in the interleaved laminate because of the shielding effect of the interleaf. Compression Strength After Impact (CSAI) could not be used for the test laminates in this project, but the Tensile Strength After Impact test provided useful results. The tensile strength after impact of the interleaved specimen was between 20%-80% more

than the baseline laminate upto impact energy of 10 ft-lb. The advantage of the interleaved specimen reduced at higher energy levels of impact.

Acknowledgements

This project has been successfully completed only because of the cooperation received from several individuals and companies that participated in its completion.

I would first like to thank my faculty advisor, Dr. O.H. Griffin, for his willingness to take up this experimental project with me despite his analytical interests. He has been very inspiring and helpful in the successful planning of this project.

I would also like to thank my committee members, Dr. E.G. Henneke and Dr. A.C. Loos who were always willing to offer their time and advice in some of the difficult situations during this project.

The staff of the Engineering Science and Mechanics Department, especially Robert Simonds, Chuck Chandler and Robert Davis were extremely helpful in offering their expertise and help in fabrication and testing of the test samples. I am very grateful to all of them.

This project also involved the cooperation of several companies; Fiberite Inc., American Cyanamid Company, Allied Fibers Technical Center, and American Research Corporation of Virginia. I am grateful to all these companies for providing materials, testing facilities and expert advice. I would like to thank the American Research Corporation of Virginia for allowing the use of the eddy current apparatus for this project. Much of the information in the chapters on eddy current scanning and interleaved composites has been taken from various textbooks and technical publications. I do not wish to take credit for any information in these chapters.

I am especially grateful to Dr. John Masters of the American Cyanamid Company for his supervision and advice. I would also like to thank Mr. Brian Waring and Wayne Brockwell of Allied Fibers for their help with the instrumented impact tests. My special thanks are also to C. P. Agrawal for helping me in preparing this manuscript.

Table of Contents

- 1.0 INTRODUCTION 1**

- 2.0 INTERLEAVED COMPOSITES 4**
- 2.1 INTRODUCTION AND BACKGROUND 4
- 2.2 IMPACT BEHAVIOR - LITERATURE REVIEW 7
- 2.3 FABRICATION OF INTERLEAVED LAMINATES 9

- 3.0 EDDY CURRENT INSPECTION TECHNIQUE 13**
- 3.1 INTRODUCTION 13
- 3.2 PHYSICAL PRINCIPLES 15
 - 3.2.1 The Lift-off effect 16
 - 3.2.2 Edge effect 18
- 3.3 INTERPRETATION OF EDDY CURRENT INDICATIONS 19
- 3.4 EDDY CURRENT INSPECTION METHOD 21
- 3.5 TYPES OF EDDY CURRENT COILS 23
 - 3.5.1 Probe coils 23
 - 3.5.2 Encircling coils 25

3.5.3	Bobbin coils	25
3.5.4	Absolute and Differential coils	25
3.6	EDDY CURRENTS IN GRAPHITE/EPOXY	26
3.7	APPLICATIONS TO TESTING OF GRAPHITE/EPOXY	27
3.7.1	Detection of damage areas due to tensile loading	27
3.7.2	Detection of embedded metallic wire.	28
3.7.3	Scanning of Impacted Graphite/epoxy Specimens.	30
3.7.4	Detection of Delaminations.	33
3.8	ADVANTAGES AND LIMITATIONS OF EDDY CURRENT SCANNING	38
4.0	EXPERIMENTAL PROGRAM	40
4.1	MATERIALS	40
4.2	SPECIMEN FABRICATION	40
4.3	INSTRUMENTED IMPACT SYSTEM	41
4.4	TEST PROGRAM AND EVALUATION SYSTEM	43
5.0	RESULTS AND DISCUSSION	46
5.1	MECHANICAL CHARACTERIZATION OF INTERLEAVED COMPOSITES	46
5.2	NON DESTRUCTIVE TEST RESULTS	51
5.2.1	Ultrasonic C-scan Results	51
5.2.2	Eddy Current Scan Results.	55
5.2.3	Residual Strength Test Results	57
6.0	CONCLUSIONS	60
7.0	FUTURE WORK	62
8.0	REFERENCES	64

9.0 APPENDIX A 68
9.1 Experimental Test Data and Non-Destructive Test Images 68

10.0 VITA 88

List of Illustrations

Figure 1. Variation of Compressive Strength After Impact (CSAI) with impact energy for baseline and interleaved laminates [3]. 8

Figure 2. Crack growth in baseline and interleaved laminates [3]. 10

Figure 3. Cured interleaved laminate and prepreg with interleaf film [3]. 12

Figure 4. Eddy current flow generated in a flat surface [17]. 17

Figure 5. Eddy current flow generated in a cylindrical object [17]. 17

Figure 6. Typical eddy current recording with no filtering [17]. 20

Figure 7. Typical eddy current recording with filtering of low frequencies [17]. 20

Figure 8. Typical eddy current recording with filtering of high frequencies [17]. 20

Figure 9. Different types of eddy current coils [17]. 24

Figure 10. Differences between absolute and differential coils [17]. 24

Figure 11. Eddy current scan of the specimen before tensile loading. 29

Figure 12. Eddy current scan of the specimen after tensile loading showing regions of damage. 29

Figure 13. Location of embedded metallic wire in the composite specimen. 31

Figure 14. Eddy current 3-D scan of the composite specimen with embedded metallic wire. . 31

Figure 15. Ultrasonic C-scan of the composite specimen with embedded metallic wire. 32

Figure 16. Location of the impact damage in the graphite/epoxy specimen. 34

Figure 17. Eddy current line scan of 5.5 ft-lb and 6.88 ft-lb impacts. 34

Figure 18. Eddy current line scan of 8.25 ft-lb and 14.67 ft-lb impacts. 35

Figure 19. Ultrasonic C-scan of the graphite/epoxy specimen with different impacts. 36

Figure 20. Eddy current 3-D scan of the impacted graphite/epoxy specimen. 36

Figure 21. Placement of simulated delaminations in the composite specimen. 37

Figure 22. Eddy current oscillograph trace of the specimen with simulated delaminations. . . 37

Figure 23. Compression Strength After Impact (CSAI) test fixture with specimen in place [3]. 45

Figure 24. Test specimen dimensions for monotonic tension and compression tests. 47

Figure 25. Ultrasonic C-scan of the T300/934 laminate(top) and IM6/1808 laminate(bottom) at 1.74 ft-lb impact. 52

Figure 26. Ultrasonic C-scan of the T300/934 laminate(top) and IM6/1808 laminate(bottom) at 3.36 ft-lb impact. 53

Figure 27. Variation of ultrasonic C-scan damage area versus impact energy for interleaved and non-interleaved laminates. 54

Figure 28. Eddy current 3-D scan for the T300/934 laminate at 4.01 ft-lb impact. 56

Figure 29. Variation of Tensile Strength After Impact (TSAI) with impact energy for interleaved and non-interleaved laminates. 58

Figure 30. Instrumented impact curves for T300/934 laminate at 0.94 ft-lb. 71

Figure 31. Instrumented impact curves for IM6/1808 laminate at 0.87 ft-lb. 71

Figure 32. Ultrasonic C-scan image for T300/934 laminate at 0.94 ft-lb. 72

Figure 33. Ultrasonic C-scan image for IM6/1808 laminate at 0.87 ft-lb. 72

Figure 34. Eddy current 3-D scan for T300/934 laminate at 0.94 ft-lb. 73

Figure 35. Instrumented impact curves for T300/934 laminate at 1.75 ft-lb. 74

Figure 36. Instrumented impact curves for IM6/1808 laminate at 1.74 ft-lb. 74

Figure 37. Ultrasonic C-scan image for T300/934 laminate at 1.75 ft-lb. 75

Figure 38. Ultrasonic C-scan image for IM6/1808 laminate at 1.74 ft-lb. 75

Figure 39. Eddy current 3-D scan for T300/934 laminate at 1.75 ft-lb. 76

Figure 40. Instrumented impact curves for T300/934 laminate at 2.42 ft-lb. 77

Figure 41. Instrumented impact curves for IM6/1808 laminate at 2.45 ft-lb. 77

Figure 42. Ultrasonic C-scan image for T300/934 laminate at 2.42 ft-lb. 78

Figure 43. Ultrasonic C-scan image for IM6/1808 laminate at 2.45 ft-lb. 78

Figure 44. Eddy current 3-D scan for T300/934 laminate at 2.42 ft-lb. 79

Figure 45. Instrumented impact curves for T300/934 laminate at 3.36 ft-lb. 80

Figure 46. Instrumented impact curves for IM6/1808 laminate at 3.38 ft-lb. 80

Figure 47. Ultrasonic C-scan image for T300/934 laminate at 3.36 ft-lb.	81
Figure 48. Ultrasonic C-scan image for IM6/1808 laminate at 3.38 ft-lb.	81
Figure 49. Eddy current 3-D scan for T300/934 laminate at 3.36 ft-lb.	82
Figure 50. Instrumented impact curves for T300/934 laminate at 4.01 ft-lb.	83
Figure 51. Instrumented impact curves for IM6/1808 laminate at 4.01 ft-lb.	83
Figure 52. Ultrasonic C-scan image for T300/934 laminate at 4.01 ft-lb.	84
Figure 53. Ultrasonic C-scan image for IM6/1808 laminate at 4.01 ft-lb.	84
Figure 54. Eddy current 3-D scan for T300/934 laminate at 4.01 ft-lb.	85
Figure 55. Instrumented Impact plot for through penetration of T300/934 laminate at 10.34 ft-lb.	86
Figure 56. Ultrasonic C-scan image for T300/934 laminate at through penetration impact of 10.34 ft-lb.	86
Figure 57. Instrumented Impact plot for through penetration of IM6/1808 laminate at 20.04 ft-lb.	87
Figure 58. Ultrasonic C-scan image for IM6/1808 laminate at through penetration impact of 20.04 ft-lb.	87

List of Tables

Table 1. EXPERIMENTAL TEST PROGRAM	44
Table 2. MONOTONIC TENSION TEST RESULTS	49
Table 3. MONOTONIC COMPRESSION TEST RESULTS	50
Table 4. INSTRUMENTED IMPACT DATA FOR THE TEST MATRIX	69
Table 5. INSTRUMENTED IMPACT DATA FOR THE TEST MATRIX (CONTINUED)	70

1.0 INTRODUCTION

The use of carbon fiber composite materials for secondary aircraft structural applications has been well established in the past decade and has increased to the point that they are being actively studied for applications to primary structures. Composite materials can be tailored to meet complex structural requirements through proper selection of fiber, resin, and laminate stacking sequence, resulting in a significant weight advantage over metallic designs.

The use of composite materials in aircraft structural components, in addition to standard design capabilities, requires a fundamental understanding of toughness and the ability to carry load after impact damage. Impact damage can result from pebbles hitting during take-off, drop of tools, foot tramping, bird hits, or enemy firing. The impact may range from low velocity, low mass impact such as tool dropping to high velocity, low mass such as bullet firing, or other combinations.

The need for more durable and damage tolerant composite materials has led to development of high strain fibers and tougher resin systems. Other methods of increasing resistance of composites to low velocity, high mass impact have been proposed [1,2]. The effect of low velocity, high mass impact on the laminate residual compressive strength has also been reported in the literature [3].

One approach toward the development of impact resistant composites is to introduce a second, separate resin system in the composite. The objective of this approach is to selectively toughen the ply interfaces, which are known to delaminate under impact. This concept, known as interleaving, is the subject of this project. A thin layer of resin is added to one side of the prepreg tape which already contains an improved tough resin system. This resin layer remains a discrete layer after the curing process [3].

This effort examines the response of an interleaved composite system under low velocity, instrumented drop weight impact and compares it with the response of a non-interleaved system. Several specimens of the two different materials were impacted at six different energy levels. The impacted specimens were then evaluated by two different non-destructive evaluation techniques and the response correlated with tension strength after impact (TSAI).

Non-destructive evaluation techniques play an important part in assessing the damage developed in composite materials. The selection of the most appropriate non-destructive technique depends on many factors such as characteristics of the imperfections, requirements of the evaluation theory, and application constraints [4]. Two non-destructive techniques, ultrasonic C-scan and eddy current scan, are used here for the evaluation of the damaged specimens.

The two materials under investigation in this project are Fiberite T300/934 (Fiberite Inc.) and Cycom IM-6/1808 (American Cyanamid Co.). A Dynatup 8200 instrumented drop weight impact system was used to impart several energy levels of impact to the specimens, with damage ranging from none to through penetration. Comparison is then made between the damage indicated by the non-destructive techniques and the residual tension and compression strengths after impact. Static

tension tests and compression tests are performed for comparing the static response of the two materials.

2.0 INTERLEAVED COMPOSITES

2.1 INTRODUCTION AND BACKGROUND

The vulnerability of composite laminates to foreign object impact damage has been the subject of investigation for some time [1]. Studies have shown that damage induced by low velocity, hard object impact can significantly reduce the residual tensile and compressive strengths of a composite structure even when the damage cannot be visually observed. The reduction in laminate residual strength is known to be greater with higher impact energies [3].

Studies have shown that damage due to impact can be significantly reduced by incorporating a thin discrete layer of a ductile resin system at ply interfaces. The introduction of a ductile interlayer between two layers of prepreg is expected to improve the fracture toughness and mechanical properties in transverse and off-axis directions without loss of longitudinal strength through three mechanisms. First, the interlayer should be able to absorb crack propagation energy and blunt the tip of a crack. Second, the interlayer is capable of relieving the stress concentration around the reinforcement, and, third, the interlayer can protect the brittle fiber surface from abrasion during processing and heal flaws on the fiber surface [5].

Interleaved composites have been a major area of research for the past few years because of their higher impact resistance. In April 1984, three independent research teams presented work performed on laminates containing discrete inner layers of toughened material seeking to improve delamination resistance. In an effort to increase laminate toughness, Raymond Krieger [6] identified the ultimate shear strain of the epoxy resin as a key parameter. Development of a new epoxy resin yielded both adequate toughness and compressive strength, yet the compression strength after impact was still not satisfactory. This led to the development of the 'interlayer concept.' Krieger pointed out two major advantages of the interlayer concept : (1) cracks intersecting an interlayer will have a reduced shear stress concentration, and, (2) the interlayer, with its large strain to failure, will not crack easily.

Subsequent research on composite interlayer systems has shown that the interlayer has performed very well in static loading [7], fatigue loading [8], and impact [9]. Hirschbuehler [10] studied the impact properties of several toughened epoxy systems and interleaved composites at higher temperatures and concluded that these systems offer improvements in impact resistance but at a sacrifice in upper use temperature (180-200 ° F), as compared to non-interleaved composites. Chang et. al. [5] studied the effects of a controlled modulus interlayer on the properties of graphite/epoxy composites and concluded that the thickness, modulus of the interlayer, and the bonding between the epoxy matrix and the interlayer were very important in determining the properties of the interlayer composite.

Chan et al [11] employed adhesive strips along and interior to the edge of a matrix dominated and fiber dominated laminate to investigate delamination arresting. He performed tension-tension ($R = 0.1$) fatigue loading with the maximum amplitude equal to 90% of the static strength. Delamination was successfully arrested by the interior adhesive strip and completely suppressed by the edge strips. Some of the interesting findings from his study are :

1. The baseline 'matrix dominated' laminate could not survive the load amplitude past 2.6 million cycles.

2. The edge strip configuration had a 7% increase in residual tensile strength after 2.6 million fatigue cycles, as compared to the baseline system.
3. At 4 million cycles, the interior strip configuration for this laminate showed a 7% increase in residual tensile strength over that of the baseline laminate.

Simonds et al [8] investigated the notched fatigue response of a quasi-isotropic laminate subjected to tension-compression ($R = -1$) fatigue. He concluded that under cyclic loading conditions, improved matrix toughness does not necessarily translate into improved mechanical performance.

The long-term response of interleaved composites has not been studied to date. An interesting question was posed by Newaz in Ref. [7], page 73, "In the case of long-term loading of the laminate in actual applications, I would be very concerned about the "interleaf" material from the standpoint of creep. Although one may improve delamination resistance of the composite, can you convince me why one should consider such laminate design for overall long-term performance?"

Several investigators have tried to answer this question. Swain et al [12] performed a series of tests called the Incremental Load Test (ILT) to investigate the long-term performance of interleaved composites as compared to other baseline laminates. This method involves loading the laminate to a constant strain which is held for a fixed period of time, allowing stress relaxation to occur. When the time period has elapsed, an incremental strain is added and the process is repeated.

Recently an analytical model for an intersecting and interlaminar crack in a laminated structure containing interlayers has been presented by Kaw and Goree [13] as a modification of the work done by Gecit and Erdogan [14].

2.2 IMPACT BEHAVIOR - LITERATURE REVIEW

Composite material systems must be designed not only to provide the requisite in-plane structural properties but also to increase durability and damage tolerance. The effectiveness of using tough resins to increase the damage tolerance has been established. A variety of test techniques has been employed to measure foreign object impact behavior. The extent of damage has been reported in terms of damage after a drop weight impact [1], impact while under a compressive load [3], and compression strength after impact [3]. All tests however, produce only comparative values of one system against another.

Residual compression strength vs impact energy for two laminates - a toughened system and a baseline system is shown in An examination of the cross-section of the impacted specimen indicates that impact causes considerable splitting and delamination of plies. This splitting and interply delamination is caused by the inability of the composite to undergo shear deformation. The thin resin layers at the ply interfaces are constrained from large shear deformation by their thinness and lack of ductility, leading to delamination. Figure 1 on page 8.

Chang et al. [5] studied the effects of thickness and modulus of the interlayer on the impact resistance of the laminate. When a very thin interlayer is applied, the interlaminar shear strength is at its maximum, and the impact resistance reaches its minimum. This is perhaps because thin, low T_g interlayer is capable of relieving the thermal stress buildup at the interface after curing, giving the effect of better adhesion between the fiber and the matrix, but the interlayer is still too thin to absorb the fracture energy or deflect the crack path. The impact strength reaches a maximum and the shear strength starts to decrease when the interlayer thickness is approximately 0.12 microns. The impact resistance and the interlaminar shear strength both drop when a thick interlayer is applied. The modulus of the interlayer shows a significant effect on the impact strength. Lower impact strengths of composites with a lower modulus interlayer were observed.

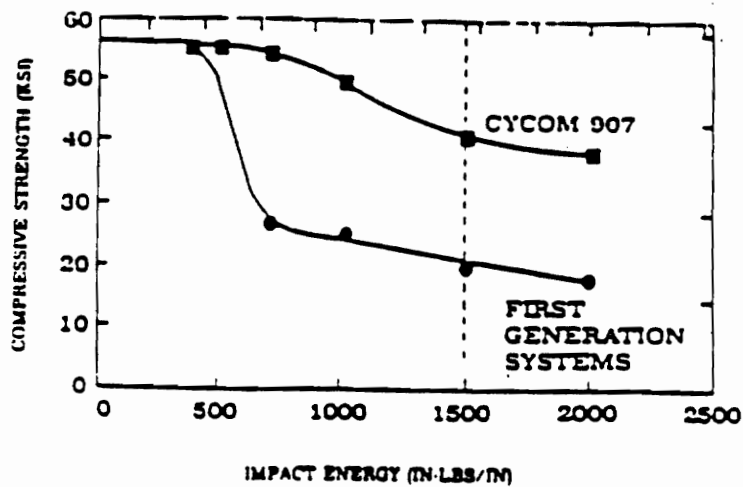


Figure 1. Variation of Compressive Strength After Impact (CSAI) with impact energy for baseline and interleaved laminates [3].

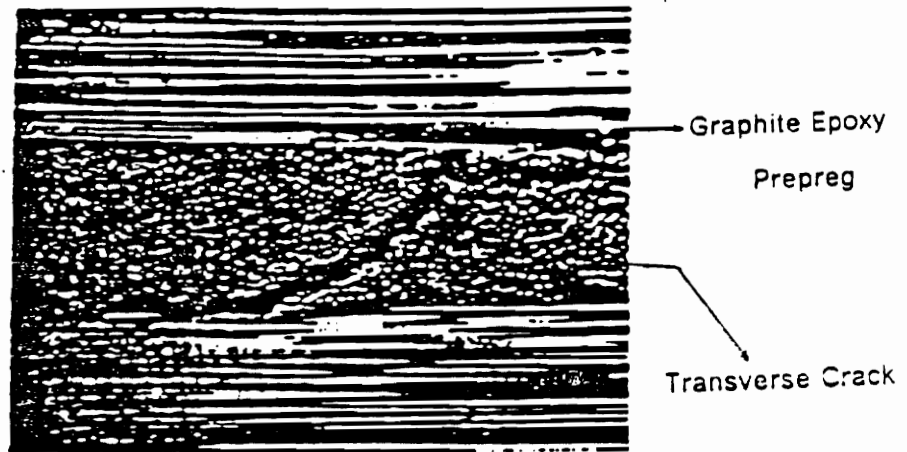
Evans and Masters [3] compared the compressive strengths of impact damaged composites with and without interleaf. The compressive strength after impact (CSAI) of the interleaved system was greater without modification of the matrix resin. The interlayer functions to suppress the initial impact damage, that is, to increase impact resistance. Smaller delamination sizes are seen in ultrasonic C-scans of interleaved panels compared to non-interleaved panels for the same energy levels of impact. Interleafing is most effective when combined with a tougher matrix system.

The basic mechanism in the interleaved laminates is the suppression of delamination at ply interfaces. Although the transverse cracks form in the material on impact, the toughened material interfaces do not delaminate. Photomicrographs, 200X, of typical transverse cracks which had developed in interleaved and baseline laminates under 3560 N-m/m (800 in-lb/in) impact are shown in Figure 2 on page 10. As can be seen in Figure 2 on page 10, while delamination developed in the baseline laminate, the interlayered laminate shows no evidence of delamination.

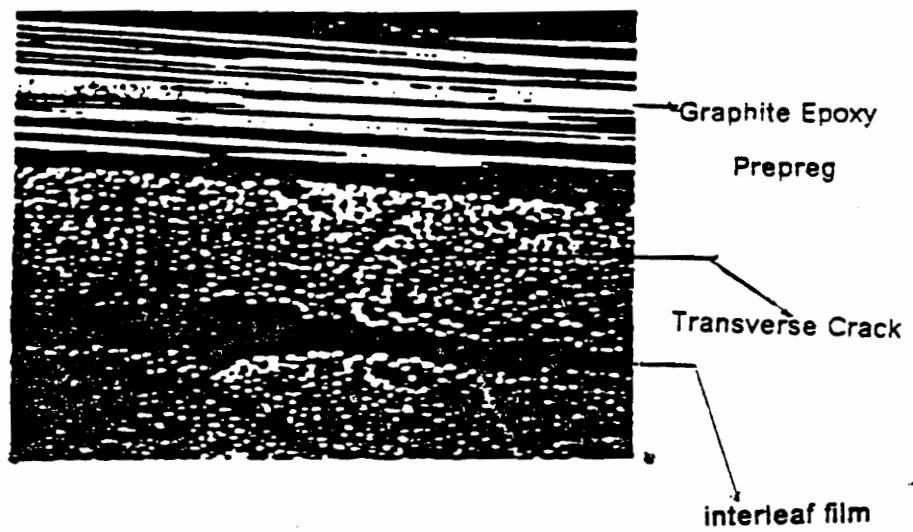
When delaminations are induced in the interlayered laminates at higher impact energy levels, they are fewer than those developed in the baseline laminates at the same energy levels.

2.3 FABRICATION OF INTERLEAVED LAMINATES

Interlayer laminates have been fabricated by two different methods. Chang et. al. [5] developed a method for the preparation of graphite fibers with an even thickness coating using an electropolymerization technique. By using graphite fibers as electrodes, and the passage of an electrical current through a suitable monomer-electrolytic medium, polymerization occurs at the fiber electrode surface. The coating is relatively uniform and the properties of the coated fiber, especially modulus, can be varied by using different monomer ratios in solutions. In addition, good chemical bonding between the interlayer and the matrix is desirable to localize energy dissipation within the interlayer and to transfer the stress to the reinforcement. The materials used in this process were methyl acrylate and acrylonitrile. The epoxy matrix used was a diethyl ether of bisphenol A cured



BASELINE LAMINATE (200 X)



INTERLAYERED LAMINATE (200 X)

Figure 2. Crack growth in baseline and interleaved laminates [3].

with 28 per hundred of methylene dianiline (MDA). Hercules AS4 graphite was used as the reinforcement.

An easier method which is more popular with the industry is to have thin discrete layers of a ductile resin between adjacent plies of the graphite/epoxy prepreg. It is important that the interlayers remain discrete after the cure process. This concept has been developed commercially by the American Cyanamid Company.

The fabrication process takes standard prepreg tape (that is, tape with a 60% fiber volume fraction) containing an improved, toughened matrix resin and adds to it a thin layer of a second interleaf resin. There are two key factors to this approach. First, the interleaf resin must have a large ultimate shear strain, and, second, it must remain a discrete layer after the laminate has been cured. Experimental results indicate that this method can significantly increase impact resistance. A photomicrograph of the interleaved laminate wherein the interlayer is seen to remain a discrete layer is shown in Figure 3 on page 12.

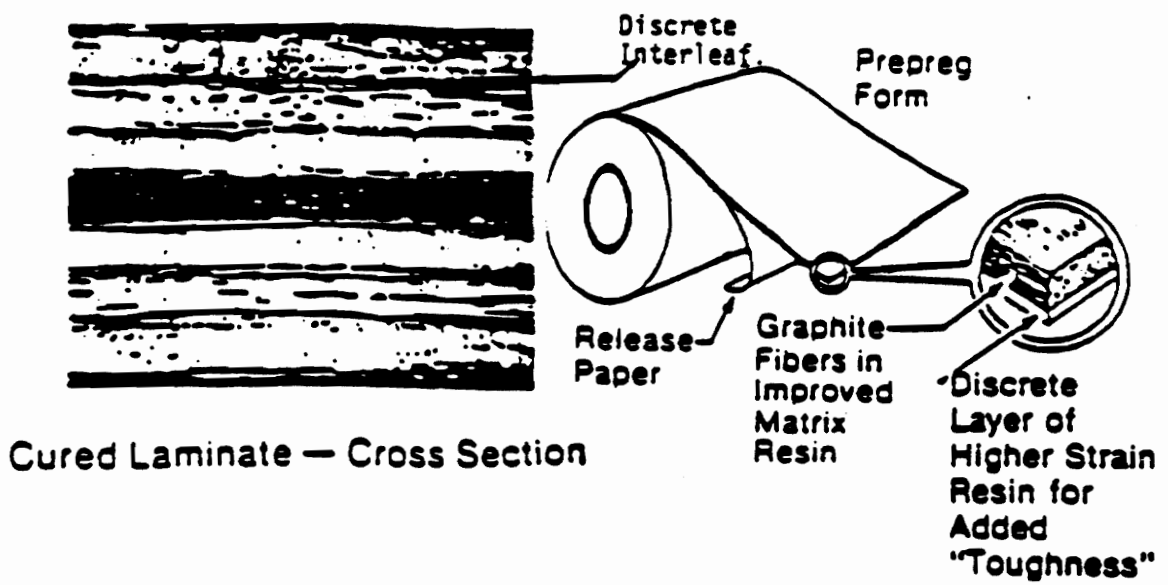


Figure 3. Cured interleaved laminate and prepreg with interleaf film [3].

3.0 EDDY CURRENT INSPECTION TECHNIQUE

3.1 INTRODUCTION

The use of graphite/epoxy composites in modern aerospace structural applications has led to the development of many non-destructive evaluation techniques for detection of damage in these composites. Ultrasonics, radiography and vibrothermography are some of the techniques currently being used in the industry. The use of eddy currents in the detection of damage in graphite/epoxy composites is currently under investigation in many research organizations [15].

The feasibility of using eddy current techniques and instrumentation in the detection of fiber breakage and delamination in graphite/epoxy composites is studied as part of this effort. Eddy current technique has shown promise as a viable non-destructive technique for damage detection of composites [16]. This technique also overcomes some of the undesirable requirements of ultra-

sonics and radiography, such as need for coupling medium and irradiation effects, giving sufficiently good results at the same time. It lends itself very easily to automation and hence data processing with the help of computers is made easy.

Eddy current testing is a method of locating surface or subsurface flaws in electrically conductive materials, and for evaluating such material characteristics as electrical conductivity, metallic coating thickness, hardness, and other conditions. The test article is brought into a time varying electromagnetic field that induces electric current. Typical currents of this sort resemble in form the eddies in flowing streams of turbulent waters; hence, they are called eddy currents. The amount of electric current flowing in these eddies is determined by the electrical conductivity of the test object as well as the frequency and amplitude of the applied electromagnetic field. These eddy currents in turn create their own electromagnetic field, which may be sensed either through its effect on the primary excitation coil or by means of an independent sensor. In non-ferromagnetic materials, the secondary electromagnetic field depends simply upon the eddy currents [18].

The first mention of eddy current-related non-destructive testing appears to be that of D. E. Hughes, who in 1879 used the sound of a ticking clock, a microphone, and an induction coil to induce eddy currents in different metals and alloys. Today numerous versions of eddy current test equipment are commercially available. Much of this equipment is useful only for exploratory tests or inspecting parts of simple geometry; however, specially designed equipment is used extensively in inspection of production quantities of metal sheet, rod, pipe, and tubing.

As a non-destructive testing tool, eddy current inspection complements the other standard methods for detection of :

1. Surface and sub-surface flaws
2. Irregularities in material structure
3. Variation in chemical composition in metallurgy

Compared with liquid penetrants, eddy currents are not as sensitive to small, open flaws; however, they have the advantage over liquid penetrants in that they are faster, they do not require cleanup operations, and more importantly, they can respond to subsurface flaws. Compared with the magnetic particle method, eddy current methods are not as sensitive to small flaws, but they are effective with both non-ferromagnetic and ferromagnetic materials. Ultrasonic methods are superior to eddy current methods for resolving small flaws and detecting flaws well below the surface; however, eddy current methods do not require mechanical coupling to the specimen as does ultrasonics. The ultrasonic signal detects flaws parallel to the surface whereas the eddy current signal is governed by those which disrupt the current carrying ability of the material. This makes the two techniques complementary. Compared with radiographic methods, eddy current techniques are faster but generally not as sensitive to small, deep subsurface flaws [18].

Some of the inherent limitations of the eddy current test methods are :

1. Depth of inspection below the surface is limited by the test frequency.
2. Eddy currents are influenced by many material variables, which often yield ambiguous test results.
3. Most test equipment needs to be manned by well trained operators.
4. Data interpretation and analysis is very subjective at this stage.

3.2 PHYSICAL PRINCIPLES

Eddy currents have no sources or sinks, but flow in paths which close upon themselves [18]. A coil excited by an alternating current produces a changing magnetic field (primary field) which induces eddy currents in the test material. The eddy currents in turn generate their own magnetic field (secondary or reaction field) which interacts with the primary field, causing a change in the

impedance of the test coil. The generation of eddy currents in two simple cases is illustrated in Figure 4 on page 17 and Figure 5 on page 17.

The main factors in determining the magnitude and direction of eddy currents induced by harmonically varying magnetic fields are :

1. The geometrical shape of the applied field (harmonics).
2. The amplitude of the applied field.
3. The frequency of the applied field.
4. The geometry of the article under test.
5. The location and orientation of the test article with respect to the applied field.
6. The electrical conductivity of the test article including inhomogenities in this property.
7. The magnetic permeability of the test article.
8. Lift-off effects.
9. Edge effects.

The lift-off and edge effects have a pronounced effect on the eddy current signal. These must be eliminated or minimized before taking any data.

3.2.1 The Lift-off effect

Electromagnetic coupling between the test coil and test object is of prime importance when conducting an eddy current scan. The coupling between the test coil and the test object varies with the spacing between the two. This spacing is called *Lift-off*. The effect on the coil impedance is called the lift-off effect. The electromagnetic field is strongest near the coil and dissipates with distance from the coil. This fact causes a pronounced lift-off effect for small variations in coil-to-object spacing. As an example, a spacing change from contact to 0.001 in. will produce a lift-off effect many times greater than a spacing change from 0.010 in. to 0.011 in. Lift-off effect is generally

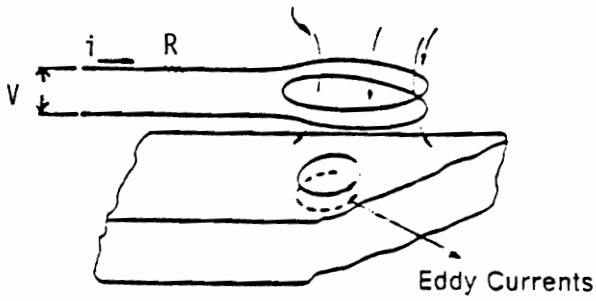


Figure 4. Eddy current flow generated in a flat surface [17].

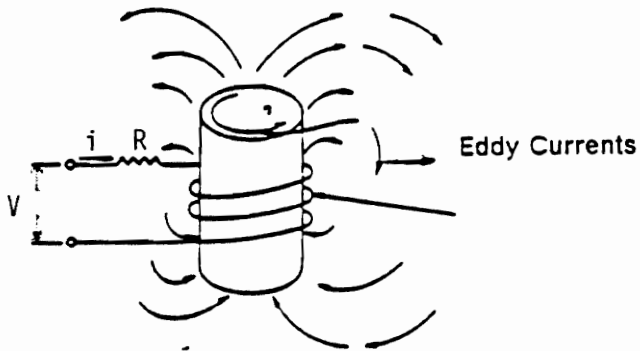


Figure 5. Eddy current flow generated in a cylindrical object [17].

undesired, and causes increased noise and reduced coupling, and results in poor measuring ability. In some instances, equipment having phase discrimination capability can readily separate lift-off effects from conductivity and other variables. Lift-off is generally kept confined to one axis of the eddy current instrument. This is done so as to keep any defect signal on the other axis. Lift-off effects must also be accounted for in cases where the probe passes over an area with a dent or a depression which may be produced as a result of damage as in the case of high energy impact.

3.2.2 Edge effect

The electromagnetic field produced by an excited test coil extends in all directions from the coil. As the geometrical boundaries of the test specimen are approached by the test coil, they are sensed by the coil prior to its arrival at the boundary. The field of the coil precedes the coil by some distance determined by the coil parameters, operating frequency, and the test object characteristics. As the coil approaches the edge of a test object, eddy currents become disrupted by the edge signal. This is known as the *edge effect*. Response to the edges of test objects can be reduced by the incorporation of magnetic shields around the test coil, by reducing the test coil diameter, or more easily by confining the scan to an area within the edges. Edge effect is a term most appropriate to the inspection of sheets or plates using a probe coil.

Even a small change in one of the coil parameters can have a marked effect on the eddy current indication. Moreover, for practical testing purposes, it is usually necessary that all except one of the parameters (the one of interest in the testing) be either rigorously controlled or accurately established.

3.3 INTERPRETATION OF EDDY CURRENT INDICATIONS

Once eddy currents have been generated and have caused changes in the original magnetizing field, the changes may be detected by one of the following methods :

1. Impedance analysis.
2. Phase analysis
3. Modulation analysis.

The Impedance analysis is the simplest and of most interest in the current work. Phase analysis and Modulation analysis are discussed in Ref [18].

Measuring only the net changes in the magnitude of the induced eddy current field, whether by observing the impedance changes in the test coil or the voltages induced in the secondary coil, is generally referred to as *Impedance analysis*. This is the least complicated method of analysis, and can be accomplished with very simple electronic circuits. Eddy current testing currently involves the use of commercially available impedance analyzers which give direct digital display of the real and imaginary components of the coil impedance. The data is then analyzed using digital computers to get meaningful interpretation of the results. The results may then be plotted to give a pictorial representation of the data.

Electronic filters are used so that results from only the variables of interest may be recorded. A typical eddy current recording without any filtering is shown in Figure 6 on page 20. For instance, a filter that will pass only high frequencies may be inserted for finding flaws such as cracks or pits. This type of recording will appear as shown in Figure 7 on page 20. On the other hand, a filter might be inserted that will pass only low frequencies to find gross defects. Such a recording may resemble Figure 8 on page 20.

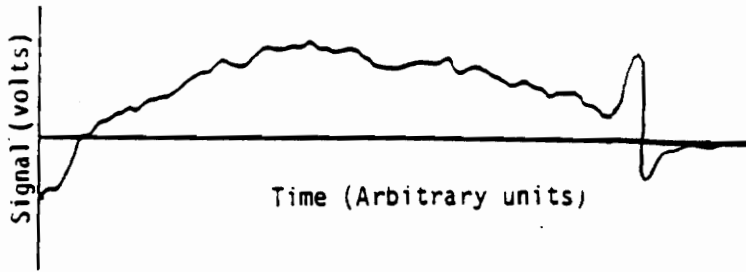


Figure 6. Typical eddy current recording with no filtering [17].

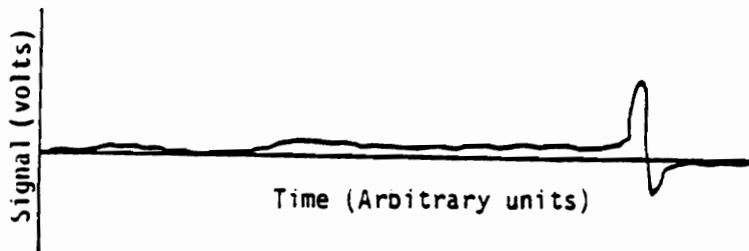


Figure 7. Typical eddy current recording with filtering of low frequencies [17].

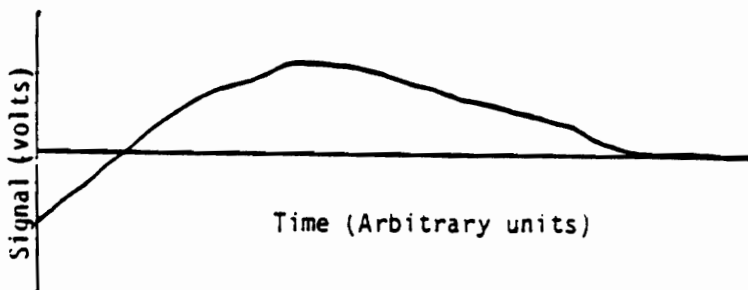


Figure 8. Typical eddy current recording with filtering of high frequencies [17].

3.4 EDDY CURRENT INSPECTION METHOD

Selecting the best eddy current technique and properly applying it requires careful planning. To insure that the inspection will have the best chance for repeatable success, the following steps should be performed.

Determining the optimum test frequency

From a knowledge of the material properties of the test article, the expected flaw size, the desired depth of penetration, and the required rate of inspection, it is possible to estimate an optimum eddy current frequency. Frequency charts that show the variation of the depth of penetration with frequency for most common metals are available [17]. A further consideration in choosing frequency is that if the test article is moving fast relative to the inspection probe or vice versa, there may not be sufficient time for a complete cycle of the applied magnetic field. Therefore there would be inadequate generation of eddy currents in the test area. Thus there is both an upper and lower limit on the test frequency.

Another expression that estimates the frequency to a sufficient degree of accuracy is given as :

$$f = \frac{1}{\sqrt{d \times c}}$$

where f = test frequency in Hertz, d = depth of penetration in cm., c = material conductivity in mhos/cm.

Thus high frequencies should be chosen for measuring surface effects whereas low frequencies should be used for subsurface effects.

Selection of Instrumentation

Once the test frequency has been established, choice of the instrument will be based on whether or not it can operate at the correct frequency. Some devices operate at a predetermined frequency, whereas others have frequency adjustments. If a single-frequency instrument is to be used, one having a frequency as close as possible to the optimum frequency for the intended test must be chosen.

Selection of Test Coil

With most commercial eddy current equipment, various sizes and shapes of test coils are supplied specifically for use with that equipment. From these coils, the operator must choose the one which is most closely suited to the geometry of the test article and is capable of establishing an eddy current pattern of a size sufficiently small to be consistent with the dimensions of the smallest flaw of interest. Whenever there are no standard coils with the test instrument or the standard transducers are of the wrong geometry for the test article, the user must design and build a transducer which must be compatible with the instrument, conform closely to the shape of the test article, and be sufficiently sensitive at the required test frequency.

Automated Scanning

For continuous inspection, if the configuration of the test article permits, the operation may be automated. Ordinarily this will require a mechanism which allows the article to move past the test probe in a repeatable fashion. Depending upon the sensitivity required, the mechanism may be either a rudimentary arrangement whereby the test article is simply moving through the magnetic field of the test probe, or for more stringent requirements, the test article may be precisely positioned and held fixed while an electromagnetic scanning system moves the probe over it. The latter ar-

arrangement reduces the possibility of the probe detecting movement or misalignment of the specimen rather than the flaws.

This arrangement is quite similar to the movement of the transducer over the test specimen as in an ultrasonic C-scan setup. The eddy current probe is aligned over the surface of the test article and the probe holder is programmed to perform a raster scan along specified dimensions. The data from the eddy current instrument is then transformed into a digital form and stored in a computer for further analysis.

3.5 TYPES OF EDDY CURRENT COILS

Eddy current test coils can be categorized into three main mechanical groups: *probe coils*, *bobbin coils*, and *encircling coils*. Different types of eddy current coils are shown in Figure 9 on page 24.

3.5.1 Probe coils

Probe coils provide a convenient method of examining the surface of a test object. Probe coils can be shaped to fit particular geometries to solve complex inspection problems. Probe coils may be used where high resolution is required by adding coil shielding.

When using a high resolution probe coil, the test object must be carefully scanned to assure complete inspection coverage. This careful scanning is very time consuming. For this reason, probe coil inspections are usually limited to critical areas. Probe coils are used extensively in aircraft inspection for crack detection near fasteners and fastener holes.

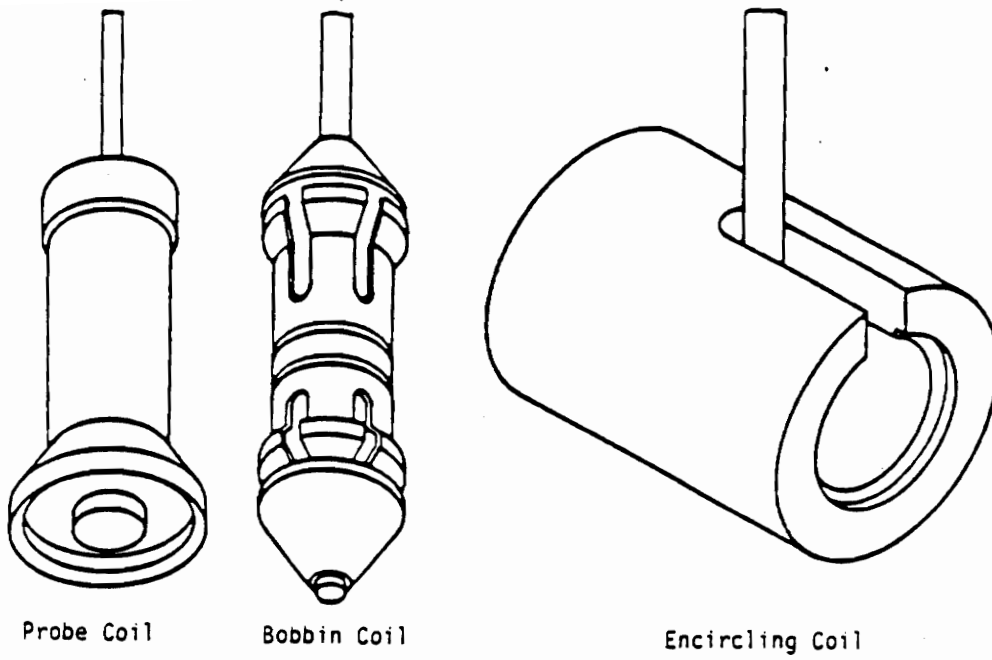


Figure 9. Different types of eddy current coils [17].

		ABSOLUTE	DIFFERENTIAL
ENCIRCLING COILS	SINGLE		
	DOUBLE		
BOBBIN COILS			
PROBE COILS	SINGLE		
	DOUBLE		

Figure 10. Differences between absolute and differential coils [17].

3.5.2 Encircling coils

Encircling coil is a term commonly used to describe a coil that surrounds the test object. Encircling coils are primarily used to inspect tubular and bar shaped products.

3.5.3 Bobbin coils

Bobbin coils are used to inspect from the inside diameter or bore of a tubular test object. Bobbin coils are inserted and withdrawn from the tube by long semiflexible shafts or simply blown in with air and retrieved with an attached pull cable.

3.5.4 Absolute and Differential coils

There is another kind of classification used for eddy current coils. These additional classifications are determined by how the coils are electrically connected. The two main categories are *absolute* and *differential*. Figure 10 on page 24 shows the differences between absolute and differential coils.

Absolute coils

An absolute coil makes its measurements without direct reference or comparison to a standard as the measurement is being made. Some applications of absolute coils are measurements of conductivity, permeability, dimensions, and hardness.

Differential coils

Differential coils consist of two or more coils electrically connected to oppose each other. Short discontinuities such as cracks, pits, or other localized discontinuities with abrupt boundaries can be detected using differential coils.

3.6 EDDY CURRENTS IN GRAPHITE/EPOXY

There are two characteristics of graphite/epoxy which require modification of standard eddy current systems and techniques designed for the non-destructive testing of metals. These are the electrical resistivity and the damage characteristics. The bulk electrical resistivity of the material is not only very high (2000-20000 μ -cm), but also highly variable. The resistivity has also been found to be frequency dependent. This has been an area of significant research, but it is not yet known how the resistivity depends on various factors such as specimen layup pattern, number of plies, etc.

The high resistivity has three implications for the eddy current method. This has been addressed by Vernon [16]. First, since the depth to which eddy currents penetrate is proportional to the resistivity of the material, much greater thicknesses can be examined than are usually associated with eddy current inspection. Secondly, when the material is relatively as thin as aircraft wing skins, frequencies higher than those used in the inspection of metals are required. Ideally the eddy current skin depth should be greater than the thickness of the specimen. Finally, larger probes are required for materials having higher resistivities. Small pencil probes provide almost no response in graphite/epoxy. Special probes must be made depending on the requirements of the test.

Graphite/epoxy is a poor electrical conductor as compared to metals. However, the fibers are conducting, so the material is amenable to inspection by a properly optimized eddy current system. When a component is under tension, it is also the fibers which carry the load. Consequently damage detected by eddy currents directly affects the fiber direction tensile strength of the test article.

Besides its higher strength to weight ratio, graphite/epoxy differs from metals with respect to a number of characteristics. Composite materials are by definition inhomogeneous. Natural inhomogeneities may mask unacceptable deviations from normal material. Fabrication related defects such as weak or non-existent interlaminar bonding as well as variations in fiber density and twisted fiber tows can weaken the material and need to be detected. Damage mechanisms in

graphite/epoxy are also different from those for metals. Service-incurred damage can result from impact. Impact damage consists of varying densities of delaminations and broken fibers. The damage initially consists of delaminations at lower loads, but at higher loads fiber breakage occurs.

3.7 APPLICATIONS TO TESTING OF GRAPHITE/EPOXY

The application of eddy current testing to graphite/epoxy is presently the object of considerable research. Presented here are the results of some experiments conducted at the American Research Corporation of Virginia at Radford, Virginia, to establish the credibility of the eddy current technique. Ultrasonic C-scans are also presented for comparison.

3.7.1 Detection of damage areas due to tensile loading

The aim of this exercise is to detect the damage developed in a laminate made of woven graphite/epoxy. The damage sustained was believed to be broken fibers as a result of tensile fracture. The stacking sequence of the laminate was unknown.

Material data

Material used	- Woven fabric graphite/epoxy laminate.
specimen size	- 8" X 3" X 0.072".
Tensile strength	- 9410 lbs. loaded along the length.
Maximum strain	- 1%

The pre-scan and the post-scan of the specimen are shown in Figure 11 on page 29 and Figure 12 on page 29, respectively.

The regions of damage as shown in Figure 12 on page 29 had some broken fibers which could be visually observed. The The post-scan (eddy current scan after damage) clearly shows the ability of the eddy current scanning method to detect damage, possibly broken fibers in graphite/epoxy composites. The signal at the starting point of the pre-scan is due to the probe being out of the specimen at that point and is not a defect. The effect of the probe being too close edge is seen in the pre-scan.

3.7.2 Detection of embedded metallic wire.

The objective here was to detect a metallic wire embedded in a graphite/epoxy composite plate using eddy current and ultrasonic C-scan methods. The metallic wire was embedded up to half the length of the specimen and at the center of the thickness. The material specifications are the same as given in the case of the detection of damage in tensile failure.

It is clear from the eddy current scan that embedded metallic wires can be detected. This may be due to the very high change in impedance levels from the metallic wire to the graphite/epoxy. The ultrasonic C-scan is also sufficiently accurate in determining the position of the embedded wire. It is different from the eddy current scan in that it cannot estimate the difference in material properties, which can be done using eddy currents as each metal has a specific response due to its specific conductivity and permeability values. The location of the embedded wire in the laminate is shown in Figure 13 on page 31, the eddy current scan is shown in Figure 14 on page 31, and the ultrasonic C-scan is seen in Figure 15 on page 32.

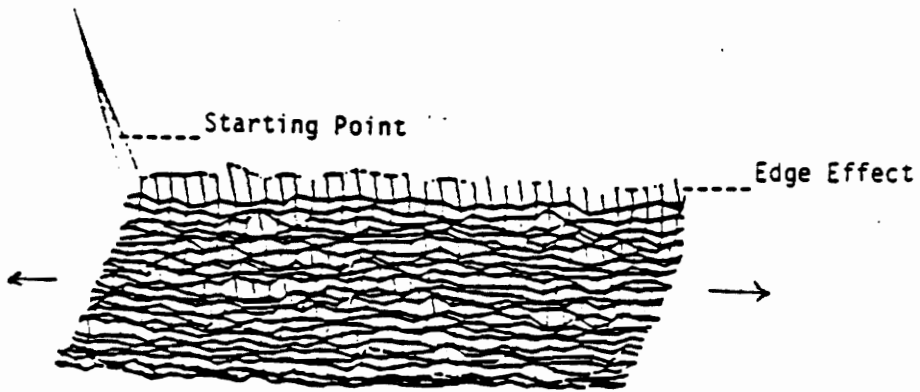


Figure 11. Eddy current scan of the specimen before tensile loading.

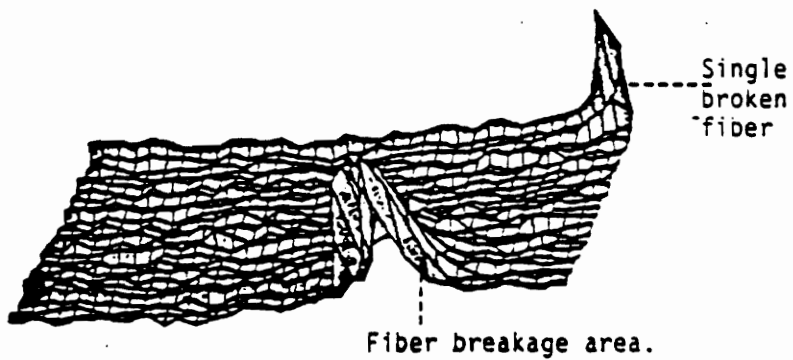


Figure 12. Eddy current scan of the specimen after tensile loading showing regions of damage.

3.7.3 Scanning of Impacted Graphite/epoxy Specimens.

The objective here was to detect damage areas resulting from impact on a graphite/epoxy laminate. The specimen is scanned using eddy current and ultrasonics and a comparative study is made. The eddy current scan was produced after filtering out the high frequencies. Eddy current line scans showing the output as response voltage versus position are also made.

Material specifications

- Material used - Hercules AS4/3501-6 prepreg cloth.
- Specimen size - 5.5" X 5.5" X 0.042"
- Stacking sequence - [0/90]_{2s}
- Tensile strength - 7900 lbs.
- impact energy levels - 5.5 , 6.88, 8.25 and 14.66 lb-ft.

The specimens were impacted using a spherical stainless steel impactor of one pound weight. It was dropped from different heights on to the specimen which was placed on a flat surface and held rigidly along the edges. The impact energy was calculated by measuring the drop height.

It is seen that the eddy current response of the specimens impacted at different levels was significant and compares well with the ultrasonic C-scan. As can be seen in both the line scan and the 3-D plot, the response of the eddy current probe is proportional to the level of impact, whereas the ultrasonic C-scan only points out the regions of delamination. Precaution should be taken to see that all the conditions at the time of testing are consistent. The specimen, with regions of damage, is shown in Figure 16 on page 34. Eddy current line scans of the 5.5 ft-lb and 6.88 ft-lb impact sites are shown in Figure 17 on page 34. Eddy current line scans of the 8.25 ft-lb and 14.67 ft-lb impact sites are shown in Figure 18 on page 35. The line scans are taken by moving the eddy current probe

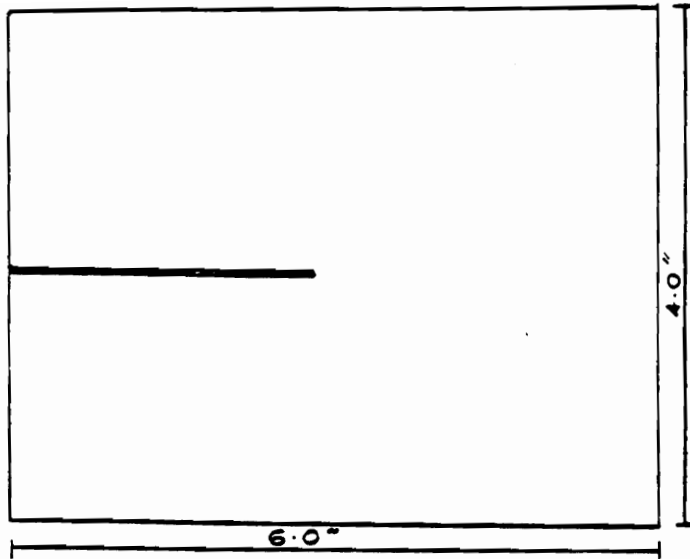


Figure 13. Location of embedded metallic wire in the composite specimen.

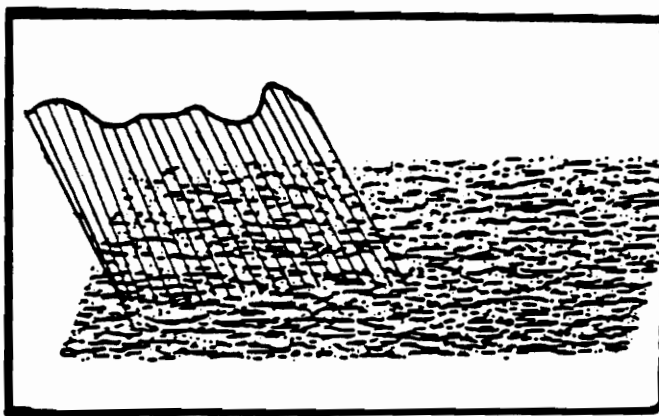


Figure 14. Eddy current 3-D scan of the composite specimen with embedded metallic wire.

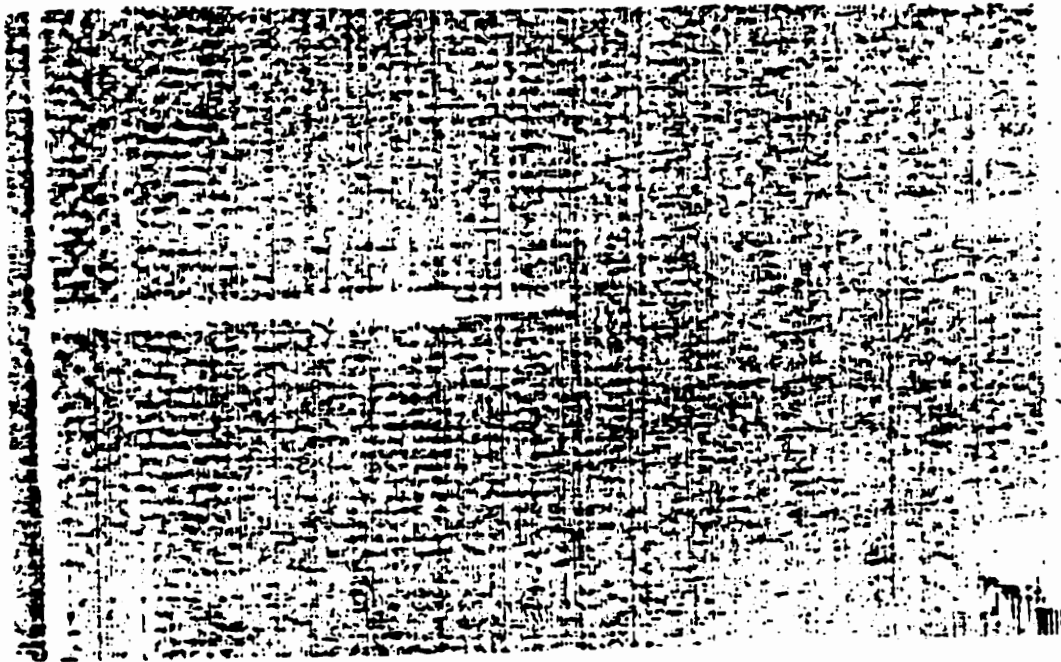


Figure 15. Ultrasonic C-scan of the composite specimen with embedded metallic wire.

over the defect location along the length of the specimen. It is taken for a period of 10 seconds to cover the entire length of the specimen. The length of the specimen used in this test was 5.5 inch. The rate used in this case was 0.5 inch/min. to cover 5.0 inches of the specimen. Ultrasonic C-scan and eddy current 3-D scan are shown in Figure 19 on page 36 and Figure 20 on page 36.

3.7.4 Detection of Delaminations.

The objective is to detect delaminations in a graphite/epoxy composite. The delaminations were induced by inserting, during layup, pieces of 8 different materials which do not bond well to the graphite/epoxy. Comparative studies of eddy current scans and ultrasonic C-scans are made.

Ultrasonics is known to be very good at detecting delaminations, and the C-scan can be taken as a reliable reference. Location of the delaminations within the specimen is shown in Figure 21 on page 37. The eddy current 3-D scan of the specimen taken out of a video display unit is shown in Figure 22 on page 37. The eddy current scan does not detect the regions of delamination very well, as only three of the eight delaminations are located. This may be due to the large difference in fiber density caused by the delamination which affects the impedance of that region and hence is shown up on the scan. Smaller delaminations are not as clearly seen.

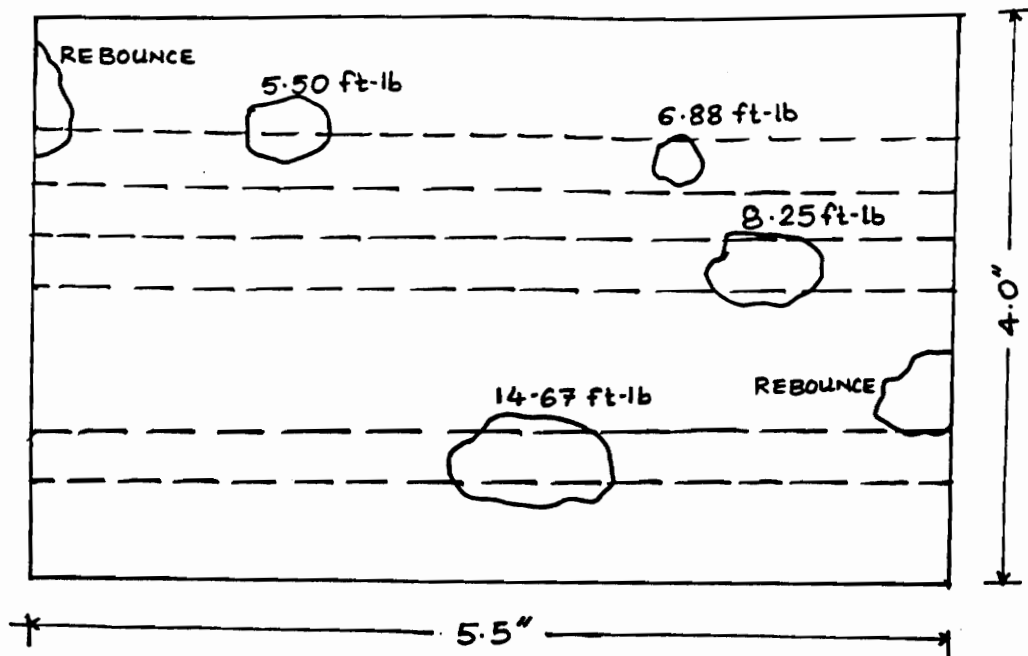


Figure 16. Location of the impact damage in the graphite/epoxy specimen.

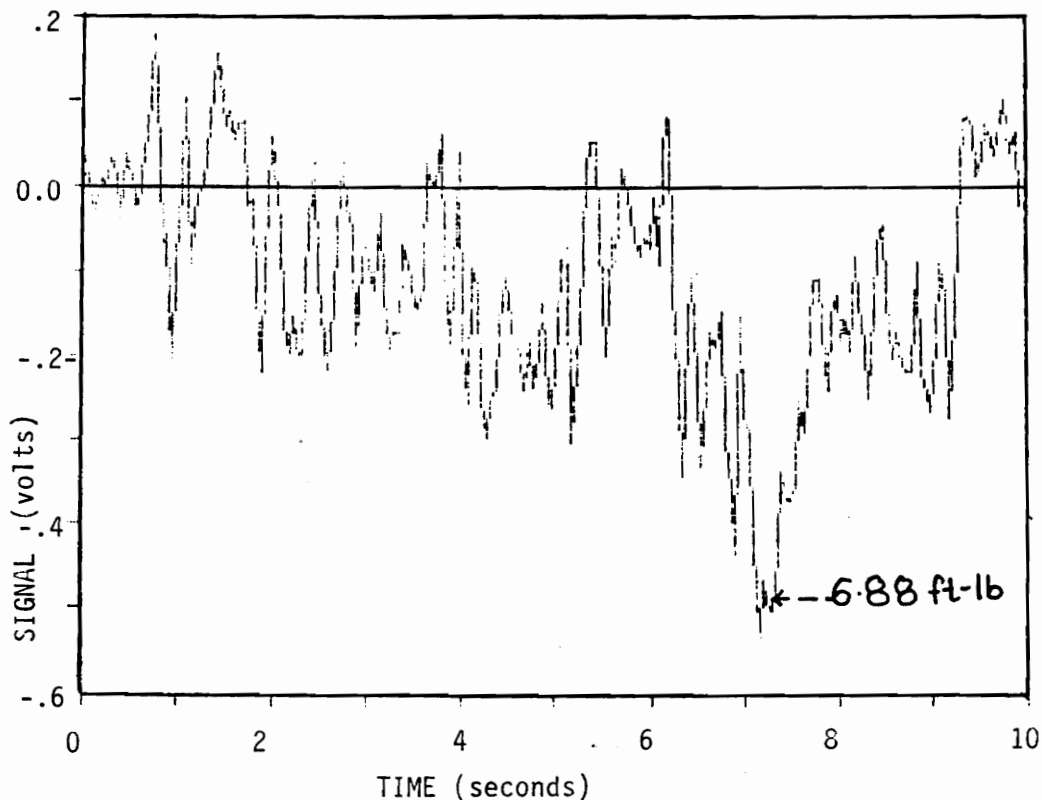


Figure 17. Eddy current line scan of 5.5 ft-lb and 6.88 ft-lb impacts.

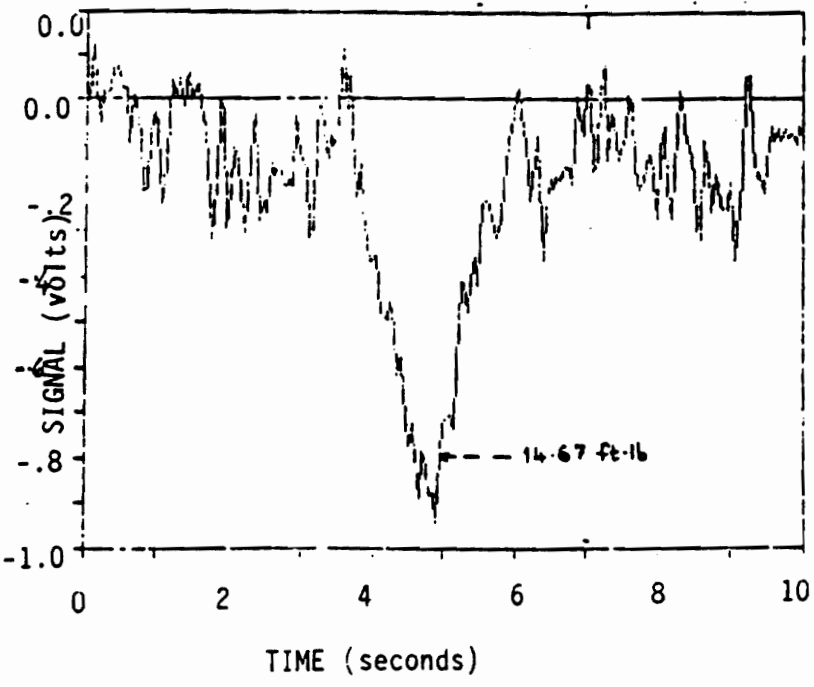
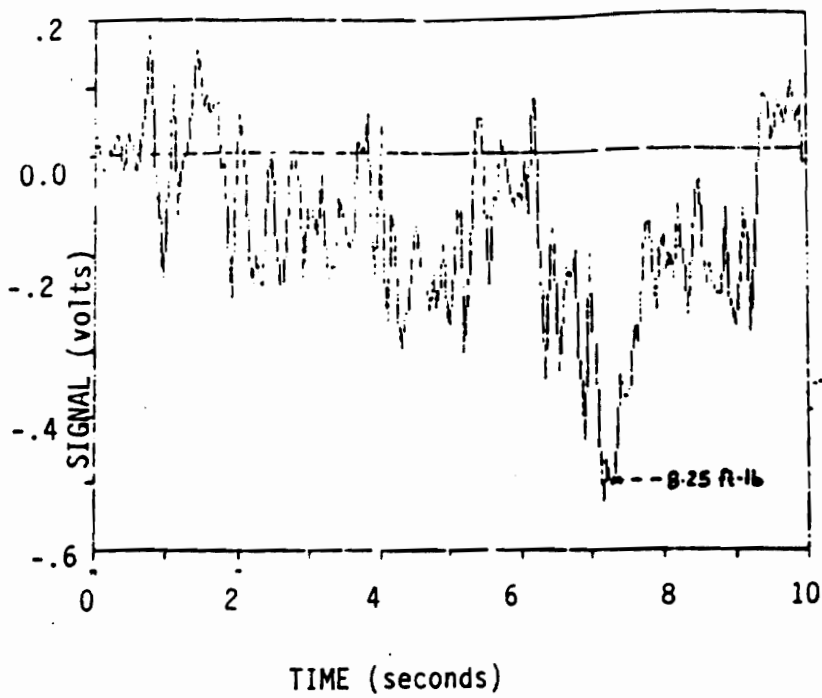


Figure 18. Eddy current line scan of 8.25 ft-lb and 14.67 ft-lb impacts.

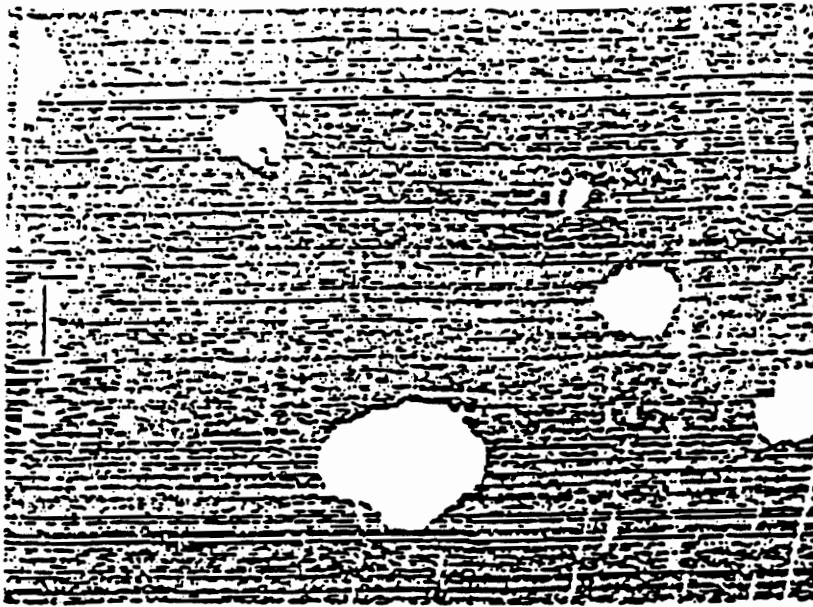


Figure 19. Ultrasonic C-scan of the graphite/epoxy specimen with different impacts.

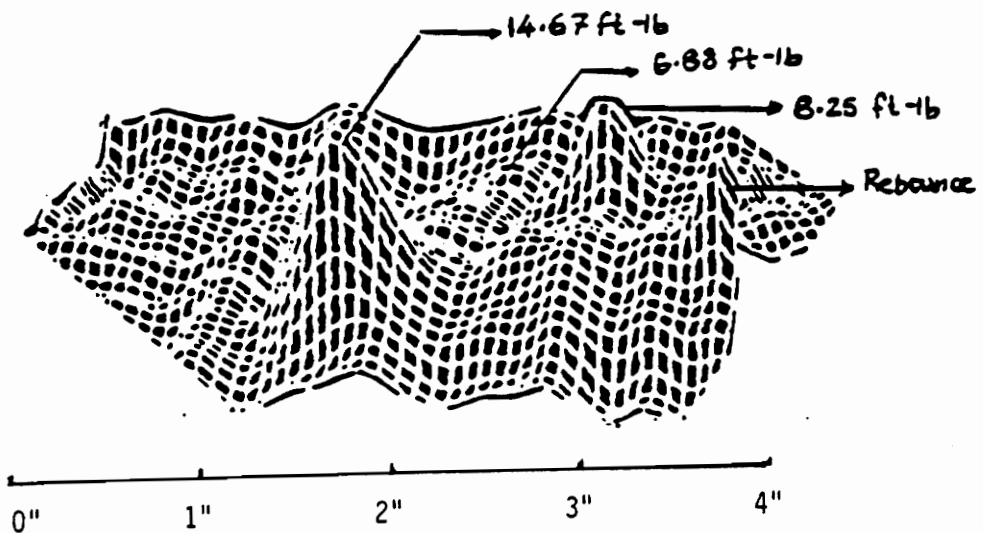


Figure 20. Eddy current 3-D scan of the impacted graphite/epoxy specimen.

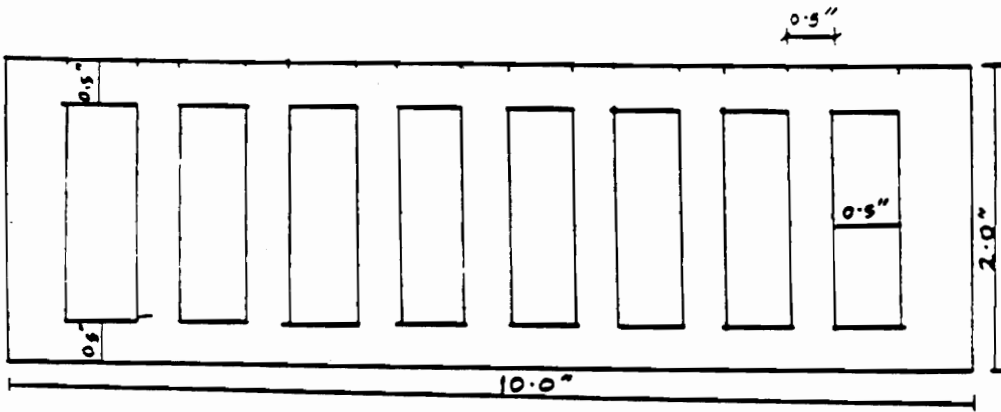


Figure 21. Placement of simulated delaminations in the composite specimen.

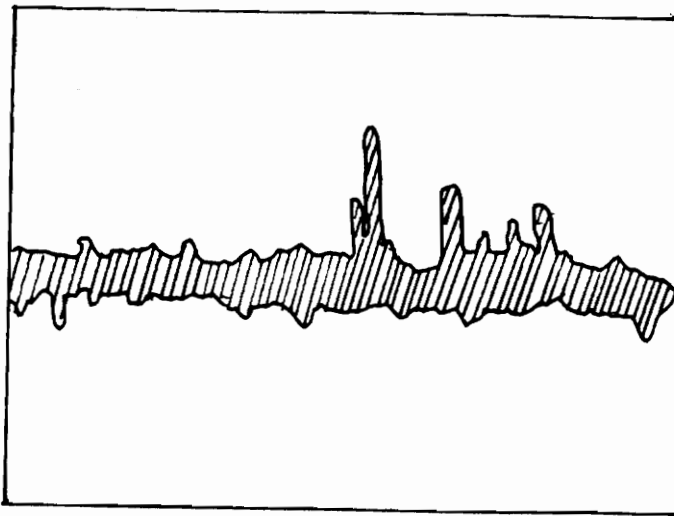


Figure 22. Eddy current oscillograph trace of the specimen with simulated delaminations.

3.8 ADVANTAGES AND LIMITATIONS OF EDDY CURRENT SCANNING

Advantages of Eddy current techniques.

1. Eddy current techniques have been found to be effective in detecting flaws. Eddy currents are particularly good at detecting flaws perpendicular to the surface. They are thus complementary to ultrasonics, which is good at detecting flaws parallel to the surface.
2. The eddy current technique is capable of inspecting at high speeds, and the indication of flaws is immediate.
3. Eddy currents seem to be effective in detecting broken fibers. The ability to detect delaminations or disbonds is questionable and requires further research.
4. Mechanical contact with the surface is desirable but not necessary. The use of a coupling medium as in ultrasonics is not necessary.
5. Eddy current scanning can easily be made portable and could be used as a "black box" technique.
6. The method lends itself to automation, and the data can be analyzed using digital computers.
7. Under controlled conditions, the eddy current technique provides an accurate measure of conductivity.

Limitations of Eddy currents

As with other non-destructive methods, eddy current technique also has certain inherent limitations.

1. The eddy current indication is influenced by a number of variables.
2. Inspection is generally restricted in depth because of skin effect.

3. The interpretation of eddy current signals is quite often subjective, as standardization has not yet been achieved.

The object of non-destructive inspection is often detection of material abnormalities and, if possible, the quantitative measurement of those abnormalities. For graphite/epoxy, these include fabrication-related weak interlaminar bonding, misplaced or twisted fibers, and porosity; and service-related delamination and broken fiber damage. Since eddy currents are carried by the graphite fibers, the method is primarily sensitive to variations in fiber density and to broken fibers. Porosity is a property of the non-conducting matrix and is not detectable by eddy currents. Large changes in fiber densities resulting from delaminations or higher porosity may be detected. Service-related defects mainly result in broken fiber damage or delaminations or both and it is the goal of the eddy current technique to detect such damage.

Before eddy current methods can be conveniently used to inspect for impact damage in graphite/epoxy at a commercial level, several problems will have to be addressed. A portable x-y scanning device interfaced with an appropriate eddy current device will have to be developed. An eddy current instrument that would give accurate readings at higher frequencies to improve depth measurements is essential.

Finally more information about the damage could be obtained by performing analysis of all the information available from the eddy current response. This will require an efficient means of controlling the different variables of the test.

4.0 EXPERIMENTAL PROGRAM

4.1 MATERIALS

The materials used in studying the impact response of interleaved composites with that of non-interleaved composites were, IM-6/1808 manufactured by American Cyanamid Company and T300/934 manufactured by Fiberite, Inc. The interleaved composite material has a thermoplastic film between every two layers of graphite/epoxy prepreg. The prepreg itself contains a toughened epoxy matrix.

4.2 SPECIMEN FABRICATION

All the specimens used for the impact testing were fabricated in the Composite Materials Fabrication Laboratory at Virginia Polytechnic Institute and State University. The prepreg was hand laid in the proper stacking sequence. A heavy roller was used to eliminate any air bubbles after each

lamina was placed. The panels were made 12 X 12 in and then cut into the required sample size of 5.5 X 4.0 in. The specimens were vacuum bagged and cured according to the cure cycle specified by the manufacturer. A thin pressure plate was placed over the specimens during the curing process. The cured specimens were cut using a high speed circular diamond coated saw, with a water jet applied while cutting. The purpose of the water jet is to cool the specimen and to keep any dust produced as a result of cutting from polluting the surroundings. The specimens were then dried and the edges were ground to make them parallel.

Ultrasonic C-scans were performed on all the specimens to ensure that there was no pre-impact delamination damage. The specimens were also scanned using the eddy current scanning technique. The specimens were then ready for instrumented impact.

4.3 INSTRUMENTED IMPACT SYSTEM

It is well known that in impact testing there frequently appear to be more variables than constants available. It is required to make the right choices to characterize the material for its ultimate use. The choices for the actual test configuration can be diverse. The specimen may be notched or unnotched, supported as a cantilever or flexural beam, flat panel, a rectangular bar, or the fabricated component. The striker or tup may be free falling or driven, and the test may be instrumented or non-instrumented. The engineer may be more interested in characterizing the impact fatigue life of the material using repeated impacts at energies less than those required for failure.

In order to define the proper test configuration for a material and its application, the stress states and likely conditions need to be identified. What constitutes failure, the mode of failure, and its likely cause need to be established. This provides the guidance necessary to determine what combination of tests is required and what environmental conditions need to be considered. In the de-

velopment of materials for new applications, instrumentation of the impact event is essential so that changes in the mechanism of failure can be quantified. Instrumentation provides data on the effective dynamic energy storage capability.

The Dynatup Model-8200 drop weight impact test machine was chosen for the purpose of the impact of the test specimens. The Model-8200 is appropriate for tests on thin sections of brittle plastics, ceramics or metals. This machine allows a wide range of test configurations so that both specimens and actual components can be tested.

The standard features of the Model-8200 include :

- Weight range from 7 pounds to 34 pounds adjustable in increments of 2.3 pounds.
- Energy range up to 96 foot-pounds.
- Drop height up to 36 inches.
- Standard base plate for clamping the flat specimen.

A General Research Corporation (GRC) 730-I data system was used to provide the energy and force versus deflection curves for the impact loading. The specimen was clamped between two oversized rectangular plates with a circular cutout of 3.0 inch diameter. The center point of the specimen was aligned with the center point of the cutout before impact. A hemispherical tup of a diameter of 0.5 inch was used for impacting the specimens.

4.4 TEST PROGRAM AND EVALUATION SYSTEM

Several specimens of the two materials were made for impacting at six different energy levels. Table 1 shows the test matrix for the experimental program.

Energy levels were chosen to vary from negligible damage to through penetration.

Two important post-impact destructive tests are the compression strength after impact (CSAI) and tension strength after impact (TSAI). The CSAI is used by aerospace organizations such as NASA [21] to determine the residual compression strength of the specimen after impact. The NASA test specimen is 8.0 inch by 10.0 inch. The thickness of the NASA specimens must be a minimum of 48 plies. It is very important to note that a specimen with lesser number of plies, or lower thickness, is not effective for this test, unless the specimen dimensions are also reduced. Premature failure due to out-of-plane buckling may result in such specimens, and thus the results may not be valid.

The TSAI is used to determine the residual tensile strength after impact in the specimen. This test can be used for specimens with lower thickness or lesser number of plies. While the compression after impact test is appropriate for laminates with delaminations, the tension test is appropriate for laminates with broken fiber damage.

A compression after impact test fixture with the specimen in place is shown in Figure 23.

This test gives the residual compression strength after impact. A static tension test is also done on the impacted specimens to get the tension strength after impact.

Ultrasonic C-scan and eddy current scans are performed before any destructive tests are done to non-destructively evaluate the extent of damage in the specimens. A comparison of the four test methods will be made to correlate the non-destructive evaluation of the damage with the residual strength of the specimens.

Table 1. EXPERIMENTAL TEST PROGRAM

TEST TYPE	MATERIAL	SPECIMEN NAME	SIZE (inches)	NO. OF SPECIMENS
STATIC TENSION	CYCOM	CT1 - CT3	10.0X0.75	3
	FIBERITE	FT1 - FT3	10.0X0.75	3
STATIC COMPRESSION	CYCOM	CC1 - CT3	1.5X1.0	3
	FIBERITE	FC1 - FC3	1.5X1.0	3
IMPACT	CYCOM	CI1 - CI23	5.5X4.0	23
		CIS1 - CIS11	5.5X3.5	11
		FI1 - FI10	5.5X4.0	10
		FIS1 - FIS3	5.5X3.5	3
CSAI	CYCOM		5.5X4.0	5
	FIBERITE		5.5X4.0	5
TSAI	CYCOM		VARIABLE	13
	FIBERITE		VARIABLE	7
ULTRASONIC C-SCAN	CYCOM	ALL	-	32
	FIBERITE	ALL		20
EDDY-CURRENT C-SCAN	CYCOM	-	-	-
	FIBERITE	F11,F14,F16		6
		F17,F19,FIS1		

All test specimens are [(0/90)_n]_s 16 ply symmetric laminates.

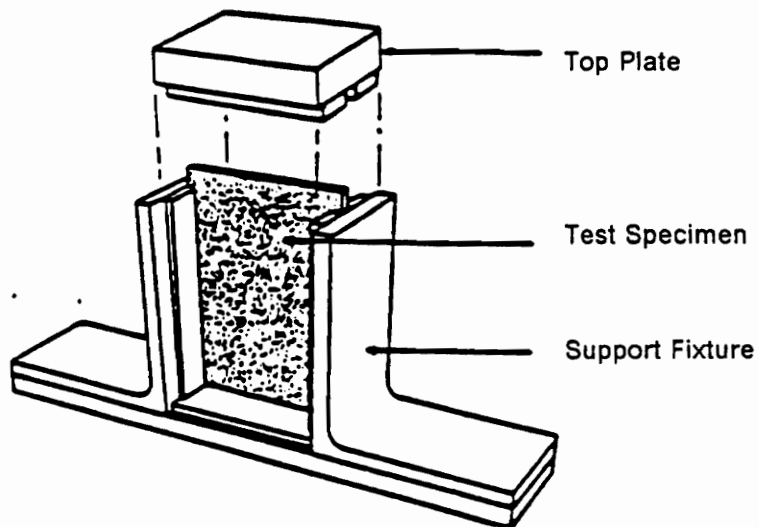


Figure 23. Compression Strength After Impact (CSAI) test fixture with specimen in place [3].

5.0 RESULTS AND DISCUSSION

5.1 MECHANICAL CHARACTERIZATION OF INTERLEAVED COMPOSITES

To study the behavior of the interlayered laminates in tension and compression, 16 layer cross-ply laminates of stacking sequence $[0/90]_{4s}$ were prepared. Standard ASTM D3090 tensile test coupons were prepared. The specimens were tabbed using fiber glass cloth tabs and gripped at the ends up to 1.5 inch. The tabs were used to prevent slipping. Compression tests were done using the test fixture designed by Z. Gurdal of Virginia Polytechnic Institute and State University [20]. The dimensions of the test specimens used for these tests are shown in Figure 24.

Most of the tensile failures of both the baseline laminate (Fiberite T300/934 prepreg) and the interleaved laminate (American Cyanamid Cycom IM6-1808/5000) occurred at the grips. A significant difference was the way in which the two specimens failed. While the baseline laminate failed with considerable fiber breakage and almost broke into two pieces, the interleaved laminate showed very little fiber breakage and maintained its integrity even on failure. In the case of the interleaved laminate, there was very little scatter of fibers.

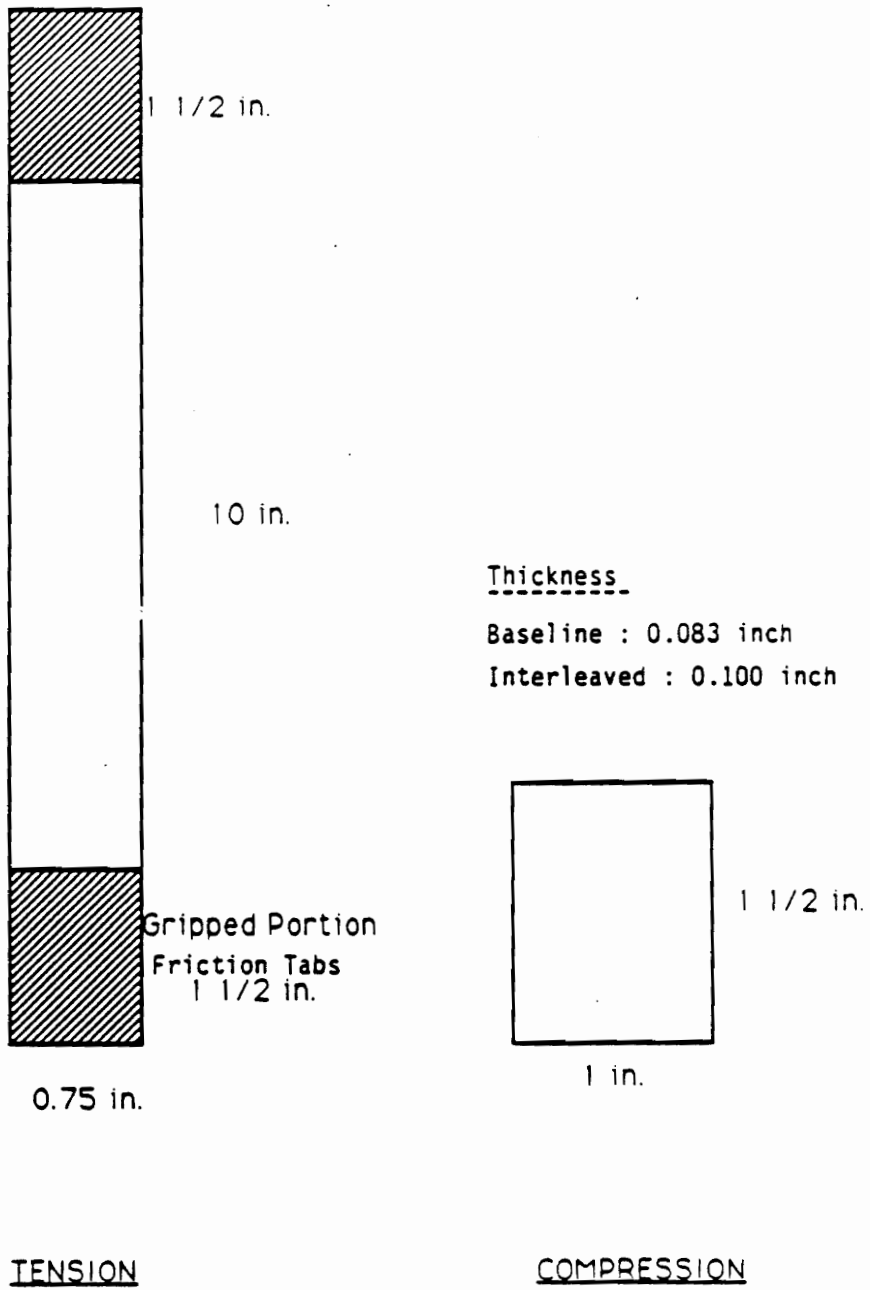


Figure 24. Test specimen dimensions for monotonic tension and compression tests.

Compression failure showed some difference for the two systems. Whereas the baseline laminates failed at the center of the specimen, the interleaved laminates failed at the bottom support. The interleaved laminates continued taking load even after the first failure had occurred. Tensile and compressive test results for the two materials are shown in Tables 2 and 3.

From the tension test results, it is seen that although the x-direction modulus did not show much change from the baseline laminate, the tensile strength increased as much as 45% for the interleaved system for a 23% increase in the cross-sectional area. The 23% increase in the cross-sectional area is because of the presence of the interlayer. The Young's modulus in the loading direction showed a decrease of only 0.7 Msi. These results and those obtained by Chan et al [11] show that the ultimate tensile strength increased considerably for the interleaved laminate over the baseline laminate. This is also confirmed by the tests performed by Soni and Kim [22] for other laminates such as $[0/\pm 45/90]_s$ and $[\{(\pm 30)_2/90\}_2]_s$. The results obtained from the monotonic tension and compression tests agreed considerably well with those obtained by Swain [12].

Compression tests done on $[0/90]_{4s}$ laminates showed a 4% decrease in ultimate strength for the interleaved composite over the baseline laminate for a 21% increase in cross-sectional area. This can possibly be explained by the presence of the ductile interlayer which is not capable of sustaining any compressive loads and hence results in the decrease of the overall compression strength of the laminate.

Table 2. MONOTONIC TENSION TEST RESULTS

BASELINE MATERIAL

SPECIMEN	FAILURE LOAD. (lbs)	E_{xx} (Msi)	STRENGTH (ksi)
ft1	6300	11.36	105
ft2	6225	11.79	100
ft3	6225	11.36	100

INTERLEAVED LAMINATE

SPECIMEN	FAILURE LOAD. (lbs)	E_{xx} (Msi)	STRENGTH (ksi)
ct1	8906	11.36	119
ct2	9750	10.40	130
ct3	8475	11.16	113

Table 3. MONOTONIC COMPRESSION TEST RESULTS

BASELINE MATERIAL

SPECIMEN	FAILURE LOAD. (lbs)	THICKNESS (in)
fc1	9449	0.083
fc2	9753	0.083
fc3	8047	0.083

INTERLEAVED LAMINATE

SPECIMEN	FAILURE LOAD. (lbs)	THICKNESS (in)
cc1	8340	0.100
cc2	9560	0.100
cc3	8297	0.100

5.2 NON DESTRUCTIVE TEST RESULTS

5.2.1 Ultrasonic C-scan Results

All the specimens were subjected to ultrasonic C-scan before and after impact. Any preexisting defect in the specimen was carefully noted before impacting it. The delamination damage in two specimens at impact energy levels of 1.74 ft-lb. and 3.36 ft-lb. is shown in Figure 25 and Figure 26. Ultrasonic C-scans depicting the delamination damage at different impact energy are shown in Appendix A. It is seen that a minimum threshold impact energy is required for the onset of delamination in any laminate. While, for the baseline laminate, the impact energy needed for the onset of delamination is 1.74 ft-lb, the interleaved laminate does not show indication of any delamination up to an impact of 2.42 ft-lb (Appendix A). The delamination has grown considerably in the baseline laminate at 3.36 ft-lb. of impact energy, whereas, for the interleaved laminate, it is about 50% less. The growth of delamination as the impact energy is increased is also found to be slower in the interleaved specimen than the baseline laminate (Appendix A).

Figure 27 is a plot of delamination area as a function of impact energy for the baseline and the interleaved laminate. For the same impact energy, it is seen that the baseline laminate shows more than double the delamination area of the interleaved laminate. While through-the-thickness penetration occurs at 10.0 ft-lb of energy for the baseline laminate, it occurs at 19 ft-lb for the interleaved laminate.

The use of a thermoplastic interleaf film alternating between every graphite/epoxy prepreg has thus shown to be very effective in suppressing the delamination damage in the test specimens. The interleaf not only delays the onset of delamination, but also considerably slows down the growth of the delamination area. The delamination seen in the interleaf laminate is significantly smaller than that in the baseline laminate. These results agree with those of Evans and Masters [3].

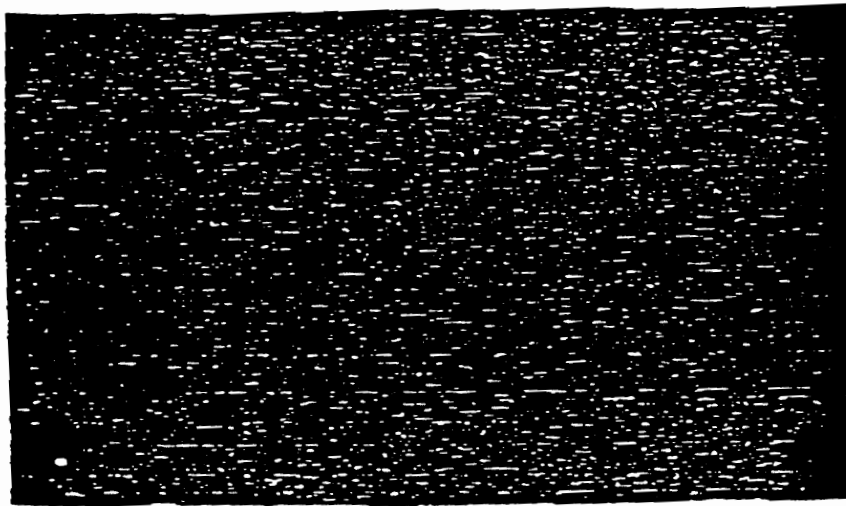
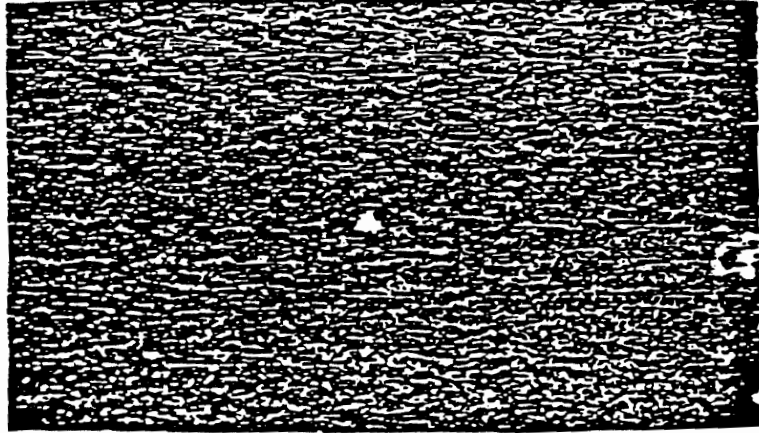


Figure 25. Ultrasonic C-scan of the T300/934 laminate(top) and IM6/1808 laminate(bottom) at 1.74 ft-lb impact.

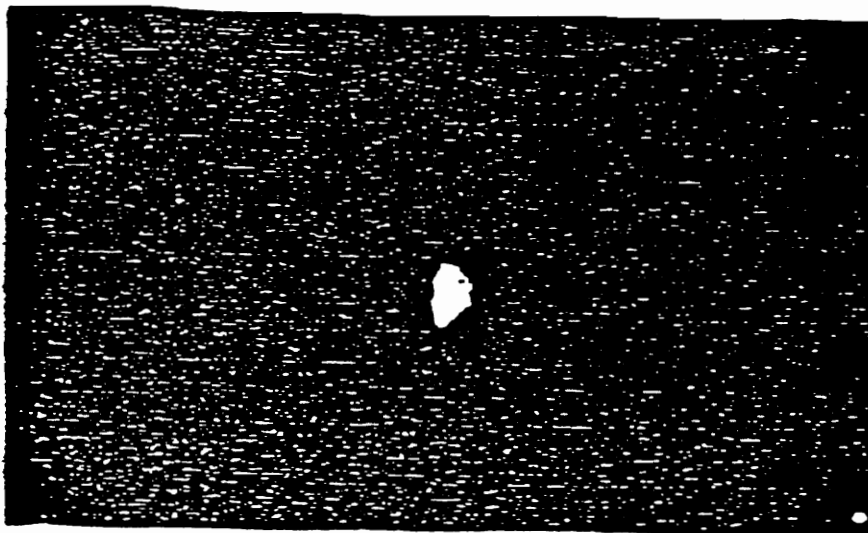
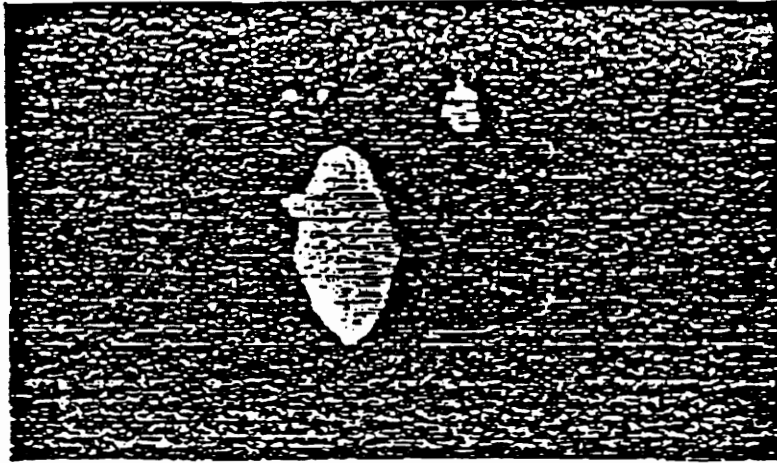


Figure 26. Ultrasonic C-scan of the T300/934 laminate(top) and IM6/1808 laminate(bottom) at 3.36 ft-lb impact.

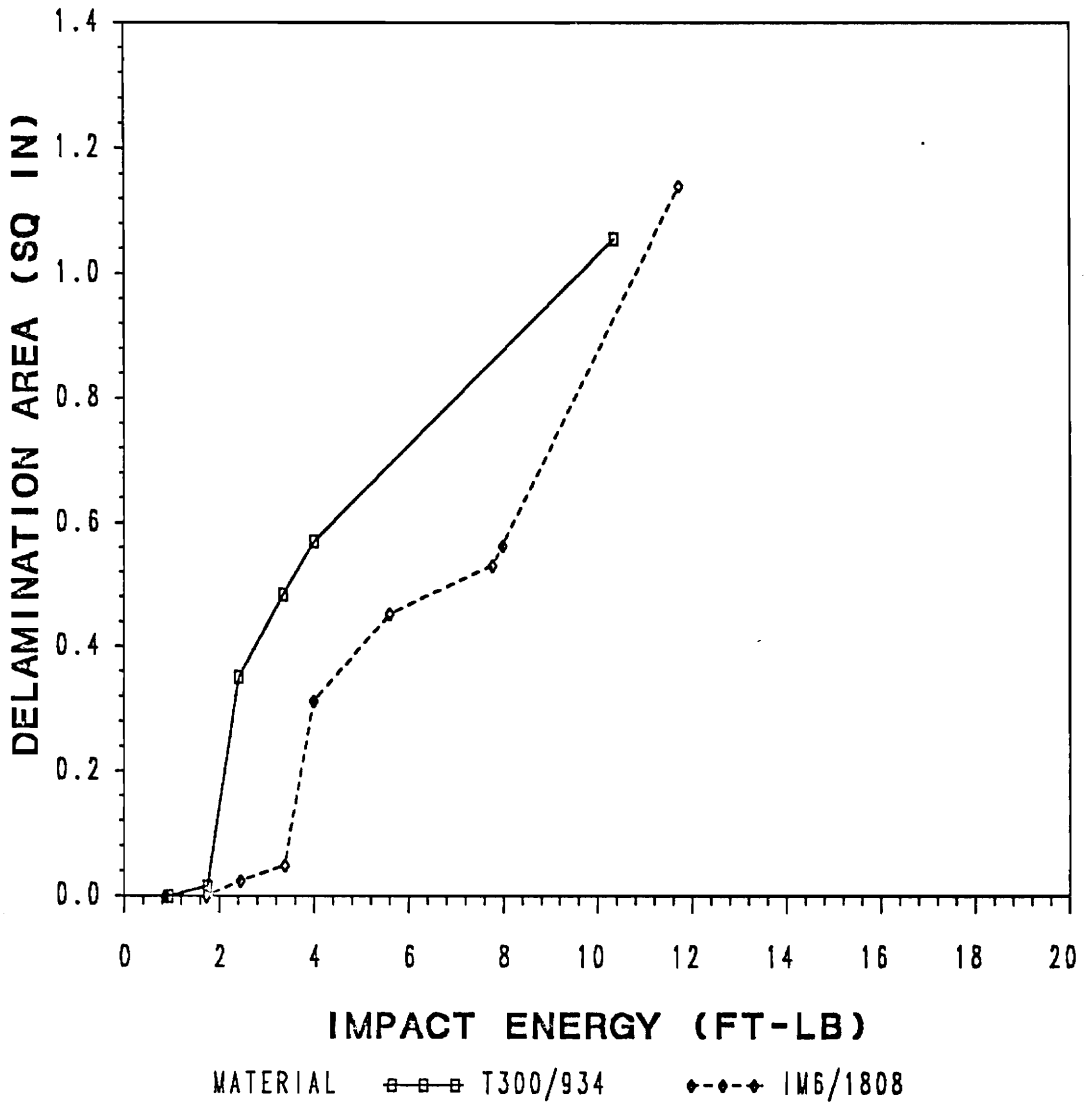


Figure 27. Variation of ultrasonic C-scan damage area versus impact energy for interleaved and non-interleaved laminates.

5.2.2 Eddy Current Scan Results.

The eddy current scan technique is being developed for the detection of broken fiber damage in graphite/epoxy composite laminates. It is applicable only to continuous conducting systems. This made the technique ineffective for the interleaved laminate, since it contains a non-conducting thermoplastic interleaf. This non-conducting interleaf acts as a shield between two conductive layers of graphite/epoxy, thus preventing a continuous generation of eddy currents for the technique to be useful. Several different probes were used, without any success.

As with ultrasonic C-scan, all the specimens were scanned with the eddy current probes before and after the impact to detect any damage. The eddy current results, as seen in Appendix A, indicate that fiber breakage does not occur in the specimen until a threshold impact energy is applied. The fiber breakage is apparent only after an impact of 4.0 ft-lb, as shown in Figure 28 for the Fiberite laminate. This has also been confirmed by the tests on Hercules AS4/3501-6 laminate. The results of those tests are shown in Chapter 3. This energy at which the fiber breakage starts in the laminate may be taken as the initiation energy for fiber breakage. An interesting observation is that the tensile load at failure after impact of the specimen is constant just about after the fiber breakage has been detected by the eddy current method.

Although the eddy current technique shows great promise as a non-destructive evaluation technique, considerable work needs to be done before making any significant conclusions from the test results. The technique is being presently developed at the American Research Corporation of Virginia.

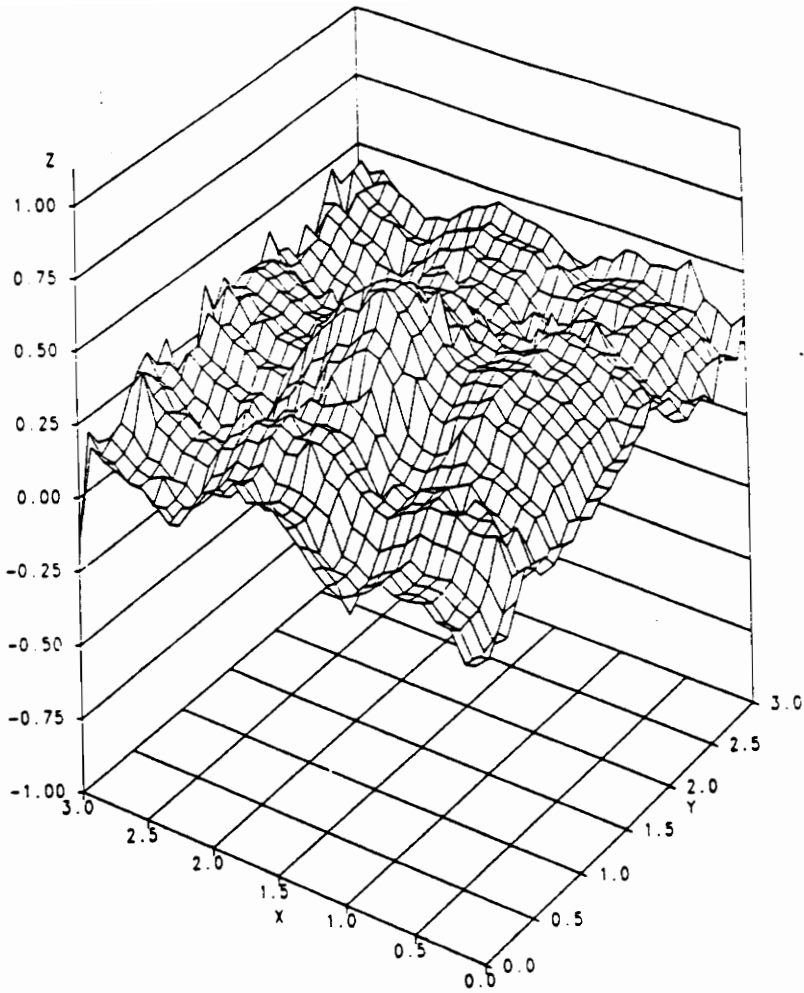


Figure 28. Eddy current 3-D scan for the T300/934 laminate at 4.01 ft-lb impact.

5.2.3 Residual Strength Test Results

Compression Strength After Impact (CSAI) Results

The compression strength after impact test is accepted by NASA, Boeing, and several other aerospace companies as an effective test for measuring the residual compression strength after impact in the specimen. The 4" X 6" CSAI specimen however, must be at least 48 plies thick to avoid any out-of-plane buckling in the specimen when the compression load is applied.

The test specimens used in this project were all 16 plies thick. Several CSAI tests done on the test specimens resulted in out-of-plane buckling of the specimen and premature failure at points different from the impact site. This was primarily attributed to the lower thickness of the specimen and possible misalignment of the test fixture, creating an eccentric loading on the specimen. The CSAI was then discontinued for this project.

Tensile Strength After Impact Results

After the failure of the CSAI to measure the residual strength, it was decided to use the monotonic tension test to failure after impact test to measure the residual tensile strength in the specimens. The test could be used to correlate the damage in the specimen with the residual tensile strength.

Monotonic tension to failure was applied to the specimen after it was impacted. Depending upon the size of the delamination in the specimen, as determined by the ultrasonic C-scan, specimens of different widths were chosen for the tension test. This was done to keep the damaged area well within the edges of the tensile specimen. The tensile strength to failure after impact was then calculated knowing the cross sectional area of the specimen. The variation of the tensile strength to failure after impact with the impact energy applied to the specimen is shown in Figure 29.

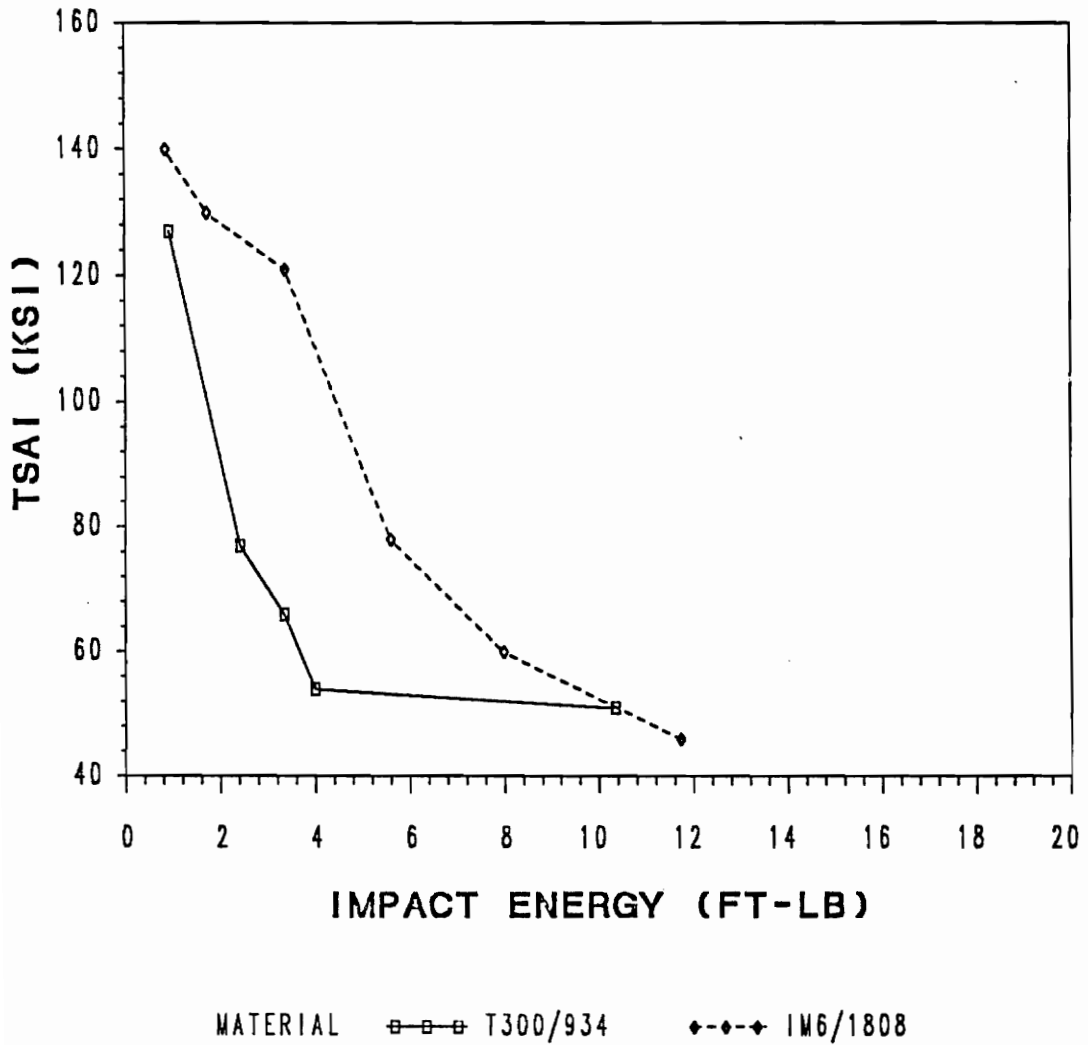


Figure 29. Variation of Tensile Strength After Impact (TSAI) with impact energy for interleaved and non-interleaved laminates.

The tensile strength after impact is plotted for both the baseline laminate and the interleaved laminate. It is seen that the interleaved laminate shows a much higher residual tensile strength after impact than the baseline laminate up to an impact energy of 10 ft-lb. At 10.0 ft-lb, the baseline laminate exhibits through the thickness penetration, whereas the energy for through penetration for the interleaved laminate was 20.04 ft-lb. The effect of the interleaf on the residual tensile strength after impact seems to reduce after an impact of 10.0 ft-lb. At lower energy levels, the interleaved laminate shows lesser fiber breakage as compared to the baseline laminate.

The interleaf is thus seen to help suppress the onset and the growth of delamination in graphite/epoxy laminates without degrading the mechanical properties of the laminate. The interleaved laminate also exhibits higher residual tensile strength as compared to the baseline laminate. Evans and Masters [3] has shown that it also increases the residual compression strength in thicker graphite/epoxy laminates.

6.0 CONCLUSIONS

This work has been primarily aimed at comparing the impact response of interleaved laminates with the baseline laminate with the help of two non-destructive quality evaluation techniques and a post-impact destructive evaluation technique. The interleaf has been very effective in increasing the impact resistance of graphite/epoxy laminates.

Several conclusions can be made from this work :

1. The use of a higher strain fiber like IM-6 and an interleaf between adjacent plies significantly increases the damage tolerance of the composite laminate, as previously found by Evans and Masters [3].
2. Instrumented impact tests provide a repeatable method of comparing the impact response of different systems.
3. The onset of delamination is delayed by the use of the thermoplastic interleaf. A significant difference in the delamination area is seen between the interleaved laminate and the baseline laminate. The growth of delamination with increasing impact energy is much slower in the interleaved laminate.

4. The eddy current technique seems to be effective in detecting fiber breakage in graphite/epoxy systems. With the probes available at the time of these tests, it was not found effective in detecting damage in the interleaved laminate because of the shielding effect of the non-conducting interleaf film.
5. For the same impact energy, the interleaf material has a much higher tensile failure load after impact than the non-interleaved material.
6. For test specimens of size 4 inch by 6 inch, the Compression Strength After Impact (CSAI) test must be used only for laminates at least 48 plies thick. Premature failure due to out-of-plane buckling is seen in laminates of lower thickness.
7. The interleaf material fails in such a way so as to cause very little fiber scatter and dust, resulting in lesser air pollution and lower chances of bodily injury.

7.0 FUTURE WORK

This effort on the comparison of the impact response of interleaved composites compared to the non-interleaved composites has created some important questions that need further research. The impact response can be improved by using a combination of a toughened matrix along with a ductile thermoplastic interleaf. The response of such a laminate can then be compared to one without the interleaf to understand the significance of the interleaf film on the impact response. More work needs to be done in the mechanical characterization of the interleaved laminate. The long term response of the interleaved composites needs to be studied.

The eddy current technique also can be further improved to detect damage in graphite/epoxy composites. Probes that are more sensitive and have higher depths of penetration could be designed. The eddy current technique can also be automated for getting instantaneous scans of the specimen to detect the presence of any flaws. More work needs to be done to prove the effectiveness of the eddy current technique in detecting fiber breakage. Probes that can penetrate the non-conducting interlayer to generate eddy currents in the conducting layers of the interleaf laminate could be designed for detecting damage in such materials.

Finally work needs to be done on the development of a damage mechanics theory which can use the data obtained from the various non-destructive techniques in a fracture mechanics model to

evaluate the residual properties of the materials. A combination of an ultrasonic and eddy current system could help in the detection and evaluation of the damage in graphite/epoxy composite materials.

8.0 REFERENCES

1. Greszczuk, L. G., "Foreign Object Impact Damage to Composites," *ASTM STP 568, American Society for Testing and Materials*, ASTM, Philadelphia, 1975.
2. Sun C. T., "Suppression of Delamination in Composite Laminates Subjected to Impact Loading," *11th Annual Mechanics of Composites Review*, Dayton, Oct. 1986, pp. 106-113.
3. Evans, R. E., and Masters, J. E., "A New Generation of Epoxy Composites for Primary Structural Applications : Materials and Mechanics ," *Toughened Composites, ASTM STP 937*, Norman J. Johnston, Ed. ASTM, Philadelphia, 1987, pp. 9-22.
4. Duke, J. C. Jr., "Weld Discontinuities-NDI Technique Selection Criteria and Factors Influencing Accuracy, Sensitivity and Reliability," *ASM Metals Handbook*, Vol. 6, 9th Edition, April 1986.

5. Chang, J., Bell, J. P., and Joseph, R., "Effects of a Controlled Modulus Interlayer Upon the Properties of Graphite/Epoxy Composites," *SAMPE Quarterly*, 18, No. 3, April 1987, pp. 39-45.
6. Krieger, R. B. Jr., "An Adhesive Interleaf to Reduce Stress Concentrations Between Plies of Structural Composites," *SAMPE Journal*, July/August 1987, pp. 30-32.
7. Hirschbuehler, K. R., "A Comparison of Several Mechanical Tests Used to Evaluate the Toughness of Composites," *Toughened Composites, ASTM STP 937*, Norman J. Johnston, Ed., ASTM, Philadelphia, 1987 pp. 61-73.
8. Simonds, R. A., Bakis, C. E., and Stinchcomb, W. W., "Effects of Matrix Toughness on Fatigue Response of Graphite Fiber Composite Laminates," *Second ASTM Symposium on Composite Materials : Fatigue and Fracture*, Cincinnati, April 1987.
9. Masters, J. E., Courter, J. L., and Evans, R. E., "Impact Fracture and Failure Suppression Using Interleaved Composites," *International SAMPE Symposium and Exhibition Series*, Volume 31, Las Vegas, April 1986, pp. 844-858.
10. Hirschbuehler, K. R., "An Improved 270 F Performance Interleaf System Having Extremely High Impact Resistance," *SAMPE Quarterly* 17 , No. 1, Oct. 1985, pp. 46-49.
11. Chan, W. S., Rogers, C., and Aker S., "Improvement of Edge Delamination Strength of Composite Laminates Using Adhesive Layers," *Composite Materials : Testing and Design (Seventh Conference) ASTM STP 893*, J. M. Whitney, Ed., American Society of Testing and Materials, Philadelphia, 1986, pp. 266-285.

12. Swain, R., "The Effect of Interlayers on the Mechanical Response of Composite Laminates Subjected to In-Plane Loading Conditions," Masters Thesis, Virginia Polytechnic and State University, Blacksburg, VA, April 1988.
13. Kaw, A. K., and Goree, J. G., "Damage Growth in composite Laminates with Interleaves," *ICCM-VI : Sixth International Conference on Composite Materials and ECCM-II : Second European Conference on Composite Materials*, F. L. Matthews, N. C. R. Buskell, J. M. Hodgkinson, and J. M. Morton, Eds., Vol 3, Imperial College, London, July 1987, pp. 146-155.
14. Gecit, M. R., and Erdogan, F., "The Effect of Adhesive Layers on the Fracture of Laminated Structures," *Journal of Engineering Materials and Technology*, Transactions of the ASME, Paper no. 77-WA/MAT-4, 100, Jan. 1978, pp. 2-9.
15. Groger, H., American Research Corporation of Virginia, Radford, VA, Personal Communication.
16. Vernon, S., "Eddy Current NDI of Graphite/Epoxy Using Ferrite Cup Core Probes," NSWC Report TR-87-148, 1988.
17. Lucero, A. L., "Eddy Current Method," ASNT Continuing Education in Non-destructive Testing, ASNT-SG-ET3-83, 1983.
18. Pasley, Richard L., and Birdwell, James A., "Eddy Current Testing," Non Destructive Testing, NASA Special Publication 5113, pp. 101-117, 1986.
19. Libby H. L., "Introduction to Electromagnetic Non-destructive Test Methods," Wiley Interscience, 1971.

20. Gurdal, Z. and Starbuck, J. M., "Compressive Characterization of Unidirectional Composite Materials," *Analytical and Testing Methodologies for Design with Advanced Composite Materials*, G. C. Sih, J.T. Pindera, and S. V. Hoa (Editors), Elsevier Science Publishers, 1988, pp. 337-347.
21. NASA/Aircraft Industry Standard Specification for Graphite Fiber/Toughened Thermoset Resin Composite Material, NASA Reference Publication 1142, June 1985.
22. Soni, S. R., and Kim, R. Y., "Analysis of Suppression of Free Edge Delamination by Introducing Adhesive Layers," *ICCM-VI : Sixth International Conference on Composite Materials and ECCM-II : Second European Conference on Composite Materials*, F. L. Matthews, N. C. R. Buskell, J. M. Hodgkinson, and J. M. Morton, Eds., Vol 3, Imperial College, London, July 1987, pp. 96-107.

9.0 APPENDIX A

9.1 Experimental Test Data and Non-Destructive Test Images

Appendix A is a collection of the instrumented impact plots showing load-deflection and energy-deflection curves recorded during the impact event. The experimental test matrix lists the details of test specimen dimensions, impact velocity, impact mass, drop height, and impact energy imparted. Ultrasonic C-scans are shown for laminates of both types; whereas eddy current plots are shown only for the T300/934 laminates.

Table 4. INSTRUMENTED IMPACT DATA FOR THE TEST MATRIX

MATERIAL	SPECIMEN NO.	THICKNESS (in)	IMPACT MASS M (lb)	DROP HEIGHT H (ft)	IMPACT VELOCITY v (ft/sec)	APPLIED KINETIC ENERGY k.e. (ft-lb)
FIBERITE	FI1	0.084	8.30	0.114	2.70	0.94
	FI2	0.083	8.30	0.109	2.64	0.90
	T300#1	0.092	8.30	0.105	2.59	0.86
CYCOM	CI1	0.100	8.30	0.105	2.59	0.86
	CI2	0.100	8.30	0.105	2.59	0.86
	CI3	0.102	8.30	0.104	2.58	0.86
	CI4	0.100	8.30	0.104	2.58	0.86
	CIS5	0.102	8.30	0.105	2.59	0.87
	CIS6	0.102	8.30	0.105	2.59	0.87
FIBERITE	FI3	0.084	8.30	0.208	3.65	1.72
	FI4	0.085	8.30	0.213	3.69	1.75
	T300#2	0.091	8.30	0.212	3.68	1.74

MATERIAL	SPECIMEN NO.	THICKNESS (in)	IMPACT MASS M (lb)	DROP HEIGHT H (ft)	IMPACT VELOCITY v (ft/sec)	APPLIED KINETIC ENERGY k.e. (ft-lb)
CYCOM	CI5	0.101	8.30	0.212	3.68	1.74
	CI6	0.100	8.30	0.210	3.67	1.74
	CI7	0.101	8.30	0.208	3.65	1.72
	CI8	0.100	8.30	0.210	3.67	1.74
	CIS1	0.102	8.30	0.208	3.65	1.72
	CYCOM#1	0.099	8.30	0.206	3.63	1.70
FIBERITE	FI5	0.085	8.30	0.299	4.38	2.47
	FI6	0.084	8.30	0.293	4.33	2.42
	T300#3	0.095	8.30	0.293	4.33	2.42
CYCOM	CI9	0.101	8.30	0.297	4.36	2.45
	CI10	0.100	8.30	0.297	4.36	2.45
	CI11	0.101	8.30	0.296	4.35	2.45

**Table 5. INSTRUMENTED IMPACT DATA FOR THE TEST MATRIX
(CONTINUED)**

MATERIAL	SPECIMEN NO.	THICKNESS (in)	IMPACT MASS M (lb)	DROP HEIGHT H (ft)	IMPACT VELOCITY v (ft/sec)	APPLIED KINETIC ENERGY k.e. (ft-lb)
CYCOM	CI12	0.101	8.30	0.296	4.35	2.44
	CIS2	0.102	8.30	0.296	4.35	2.44
	CYCOM#2	0.099	8.30	0.296	4.35	2.44
FIBERITE	FI7	0.088	8.30	0.406	5.10	3.36
	FI8	0.088	8.30	0.408	5.11	3.37
	T300#4	0.094	8.30	0.409	5.12	3.38
CYCOM	CI13	0.101	8.30	0.408	5.11	3.37
	CI14	0.101	8.30	0.409	5.12	3.38
	CI15	0.102	8.30	0.408	5.11	3.37
	CI16	0.101	8.30	0.409	5.12	3.38
	CIS3	0.102	8.30	0.405	5.09	3.35
	CYCOM#3	0.099	8.30	0.409	5.12	3.38

MATERIAL	SPECIMEN NO.	THICKNESS (in)	IMPACT MASS M (lb)	DROP HEIGHT H (ft)	IMPACT VELOCITY v (ft/sec)	APPLIED KINETIC ENERGY k.e. (ft-lb)
FIBERITE	FI9	0.091	8.30	0.487	5.58	4.01
	FIS1	0.083	8.30	0.485	5.57	4.01
CYCOM	CI17	0.100	8.30	0.478	5.53	3.95
	CI18	0.102	8.30	0.487	5.58	4.01
	CI19	0.100	8.30	0.485	5.57	4.00
	CI20	0.101	8.30	0.483	5.56	3.99
	CIS4	0.102	8.30	0.485	5.57	4.00
	CYCOM#4	0.099	8.30	0.483	5.56	3.99
FIBERITE THROUGH IMPACT	FIS2	0.082	31.36	1.52	9.87	47.47
	FIS3	0.083	31.36	1.53	9.89	47.70
CYCOM THROUGH IMPACT	CIS7	0.102	31.36	2.03	11.39	63.22
	CIS21	0.102	31.36	2.40	12.39	74.81

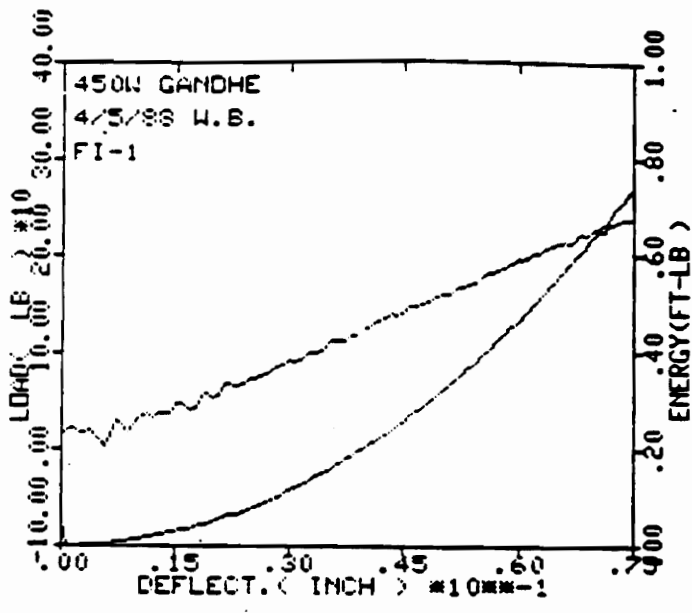


Figure 30. Instrumented impact curves for T300/934 laminate at 0.94 ft-lb.

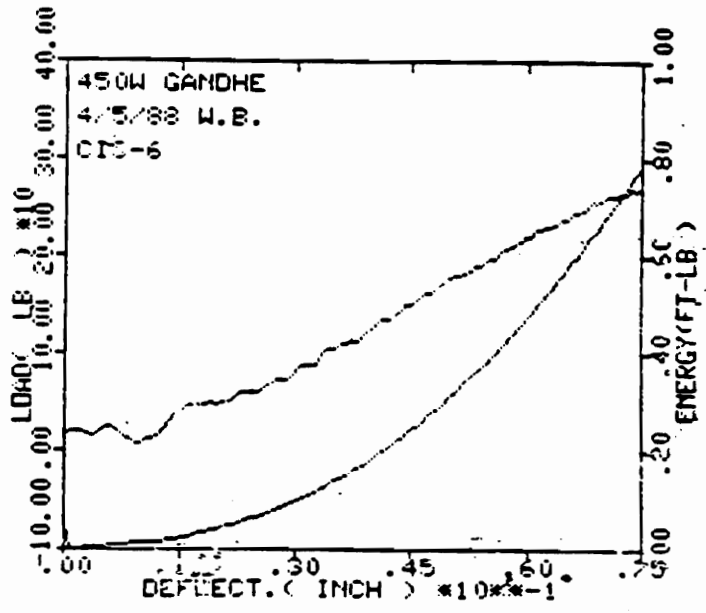


Figure 31. Instrumented impact curves for IM6/1808 laminate at 0.87 ft-lb.

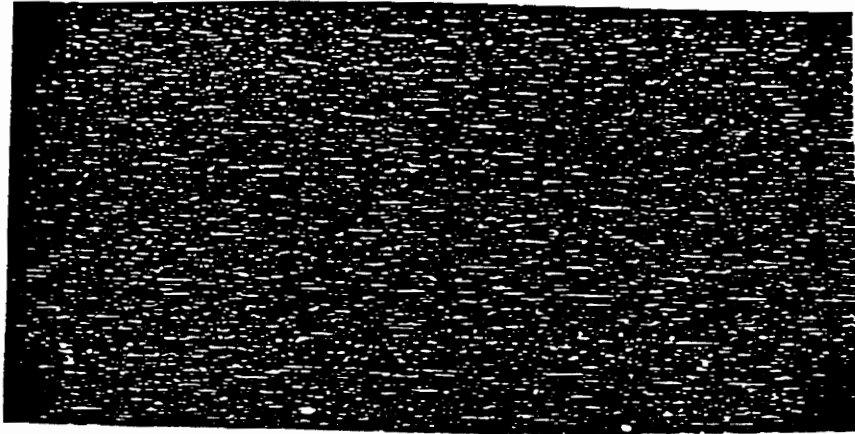


Figure 32. Ultrasonic C-scan image for T300/934 laminate at 0.94 ft-lb.

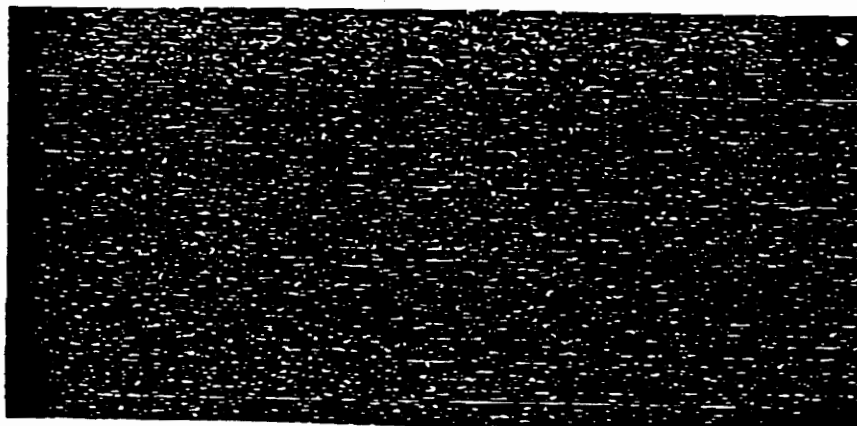


Figure 33. Ultrasonic C-scan image for IM6/1808 laminate at 0.87 ft-lb.

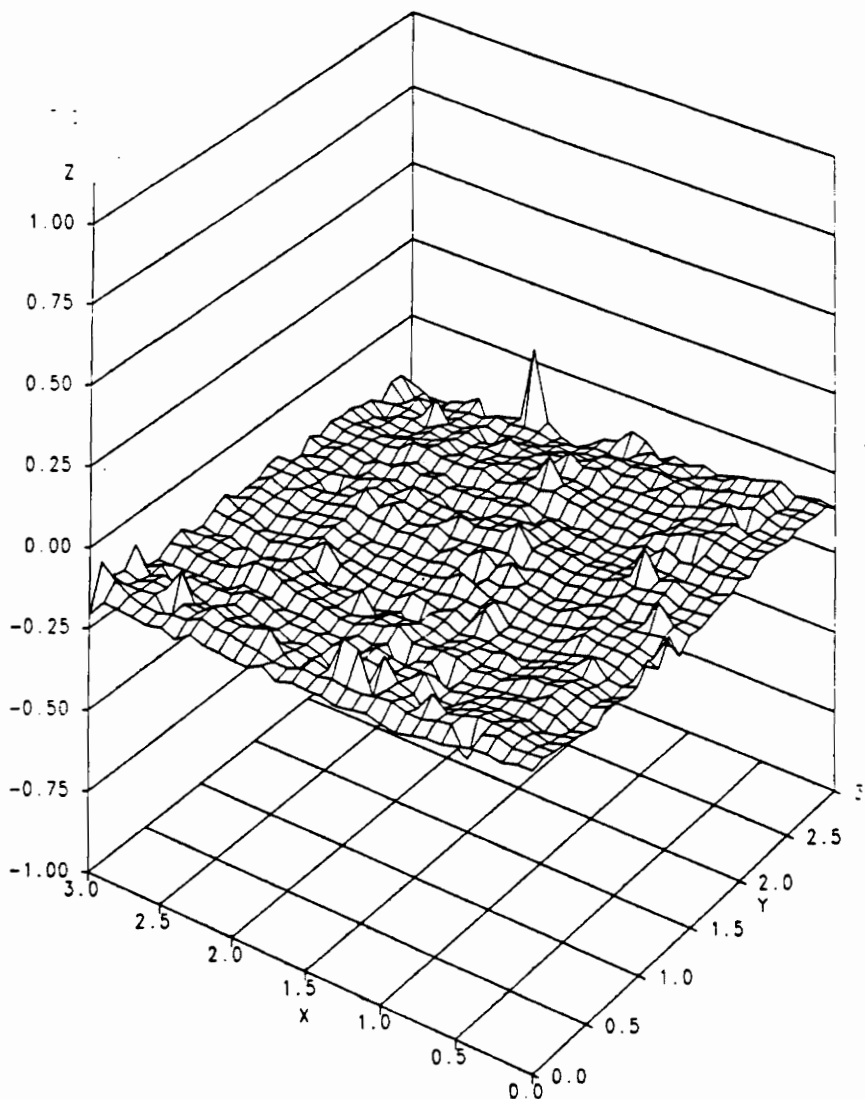


Figure 34. Eddy current 3-D scan for T300/934 laminate at 0.94 ft-lb.

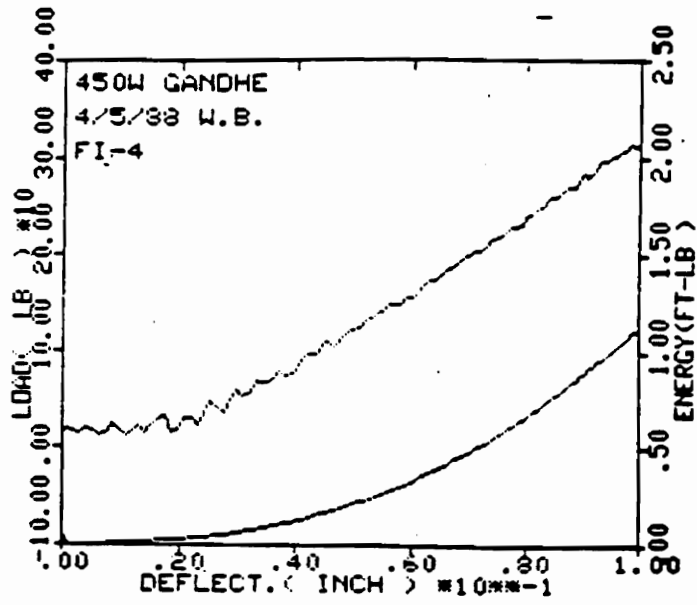


Figure 35. Instrumented impact curves for T300/934 laminate at 1.75 ft-lb.

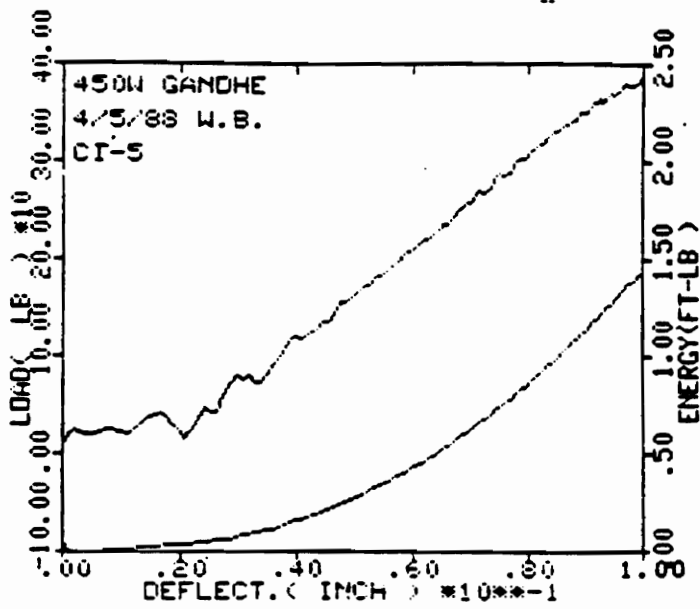


Figure 36. Instrumented impact curves for IM6/1808 laminate at 1.74 ft-lb.

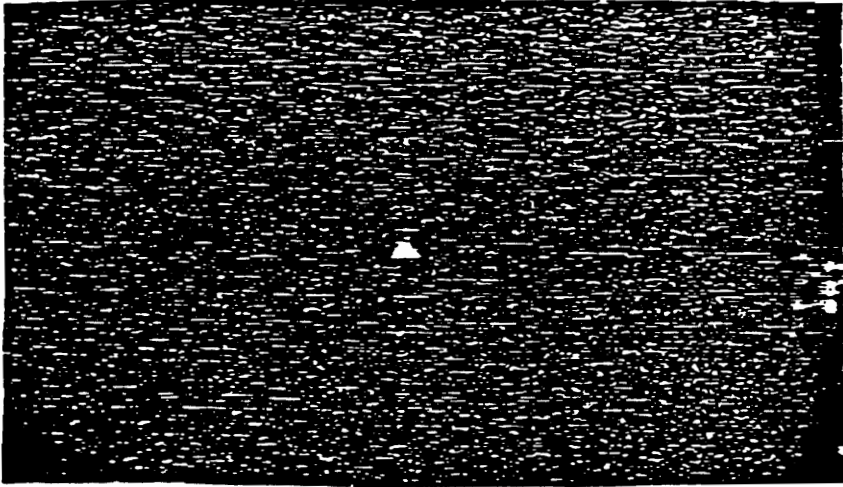


Figure 37. Ultrasonic C-scan image for T300/934 laminate at 1.75 ft-lb.

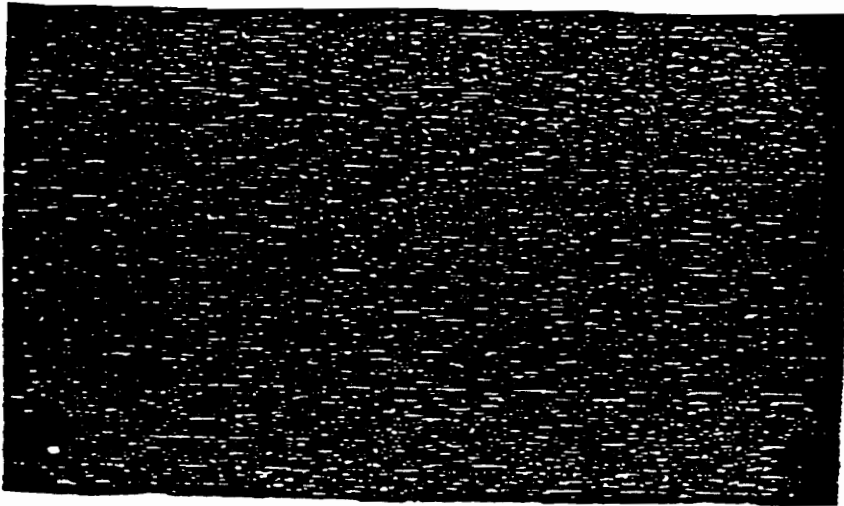


Figure 38. Ultrasonic C-scan image for IM6/1808 laminate at 1.74 ft-lb.

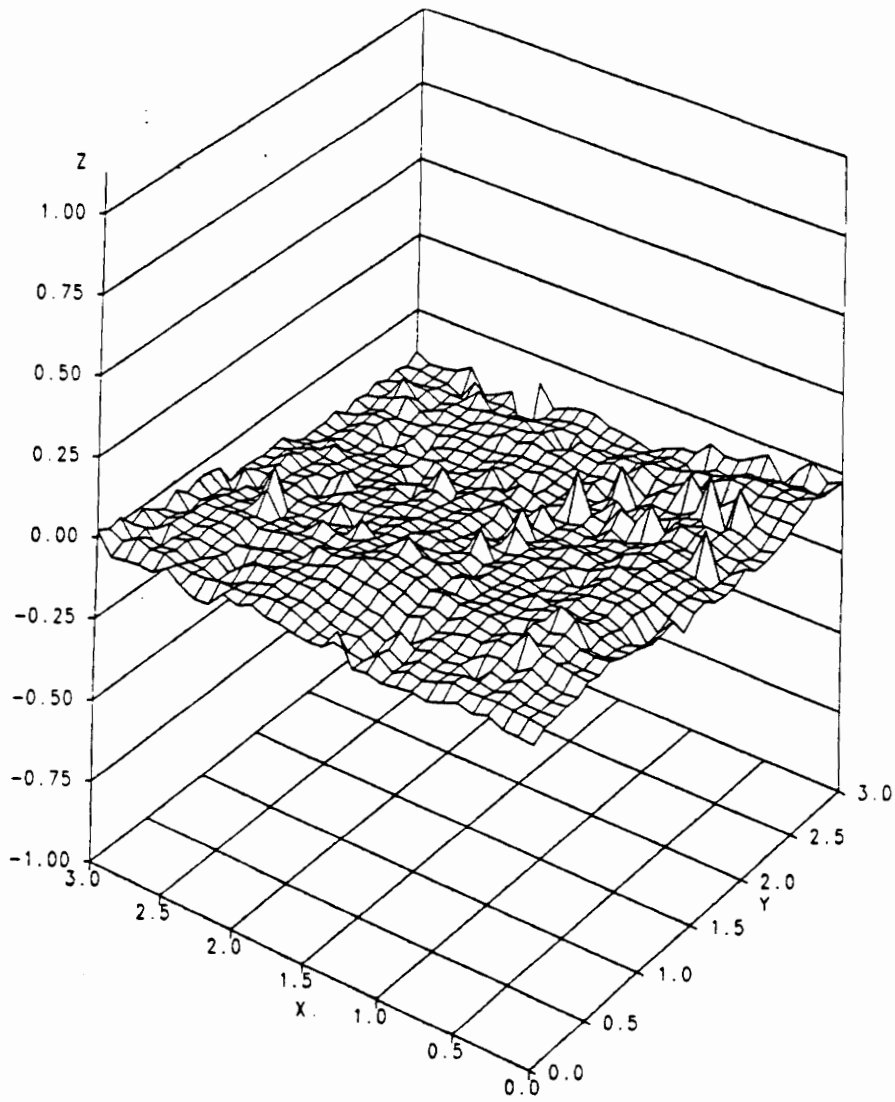


Figure 39. Eddy current 3-D scan for T300/934 laminate at 1.75 ft-lb.

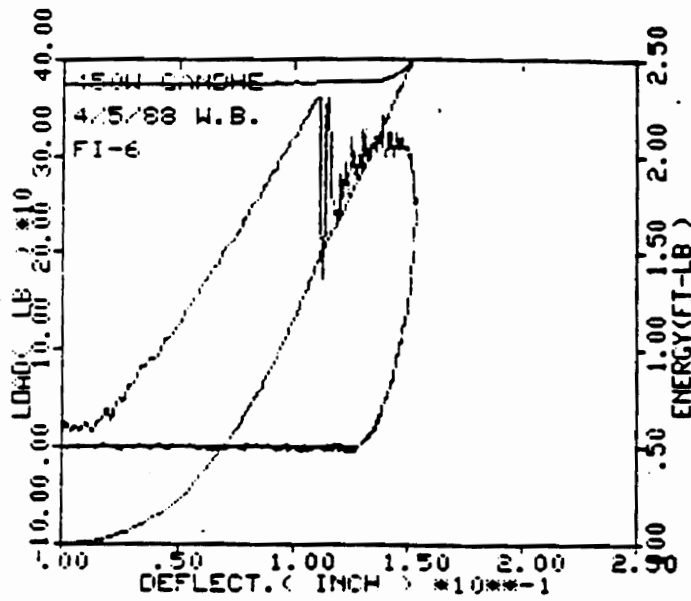


Figure 40. Instrumented impact curves for T300/934 laminate at 2.42 ft-lb.

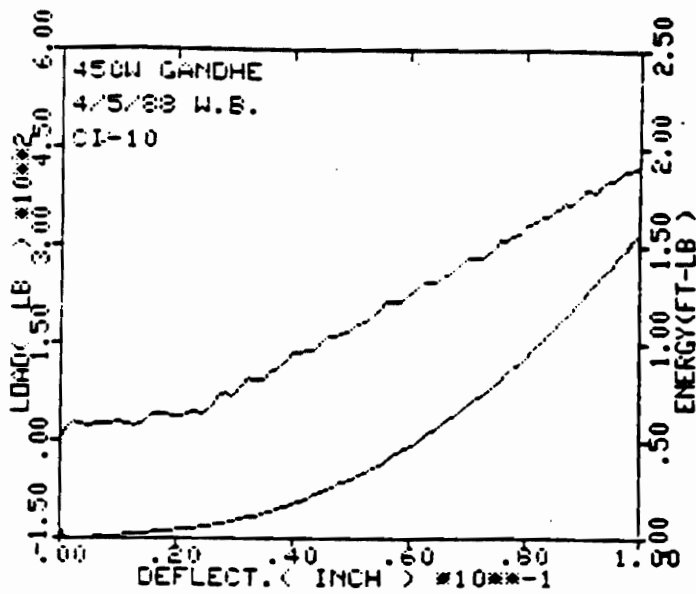


Figure 41. Instrumented impact curves for IM6/1808 laminate at 2.45 ft-lb.

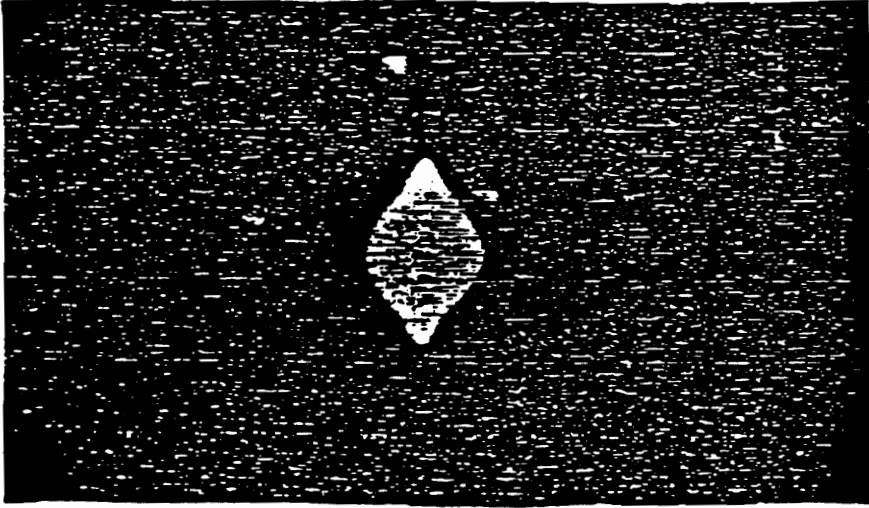


Figure 42. Ultrasonic C-scan image for T300/934 laminate at 2.42 ft-lb.

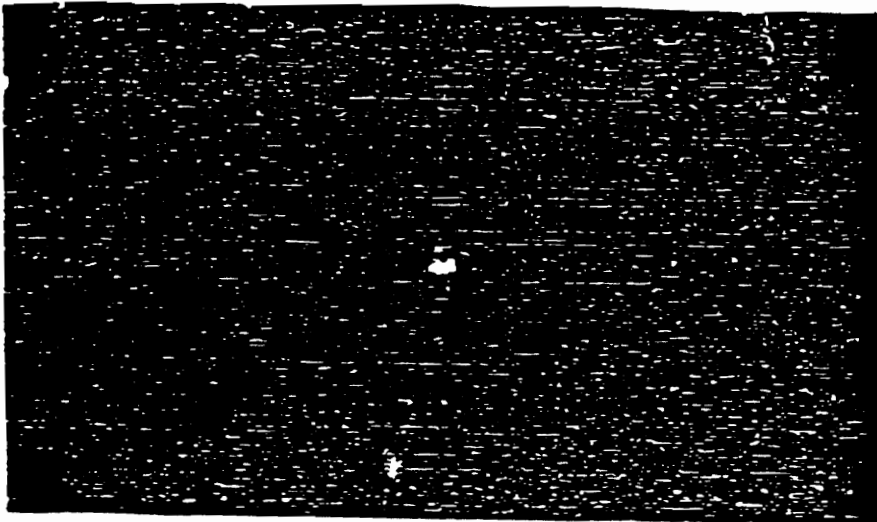


Figure 43. Ultrasonic C-scan image for IM6/1808 laminate at 2.45 ft-lb.

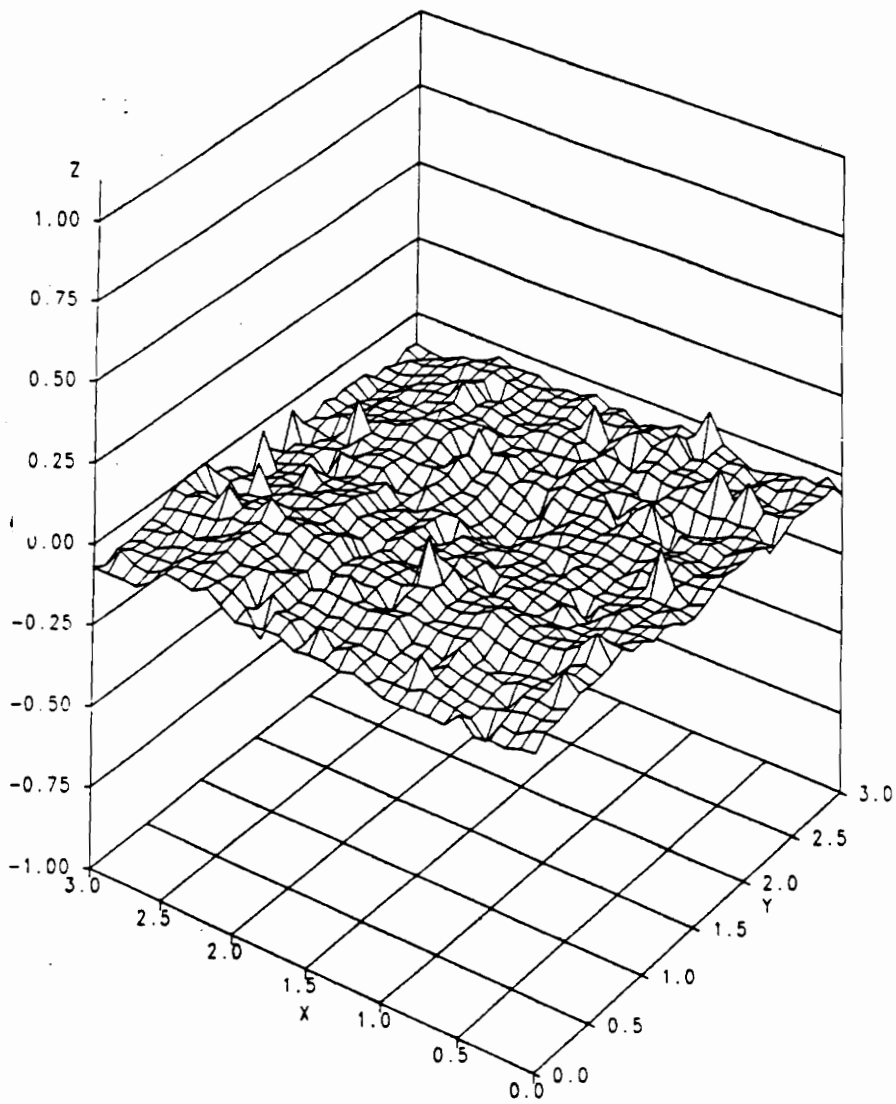


Figure 44. Eddy current 3-D scan for T300/934 laminate at 2.42 ft-lb.

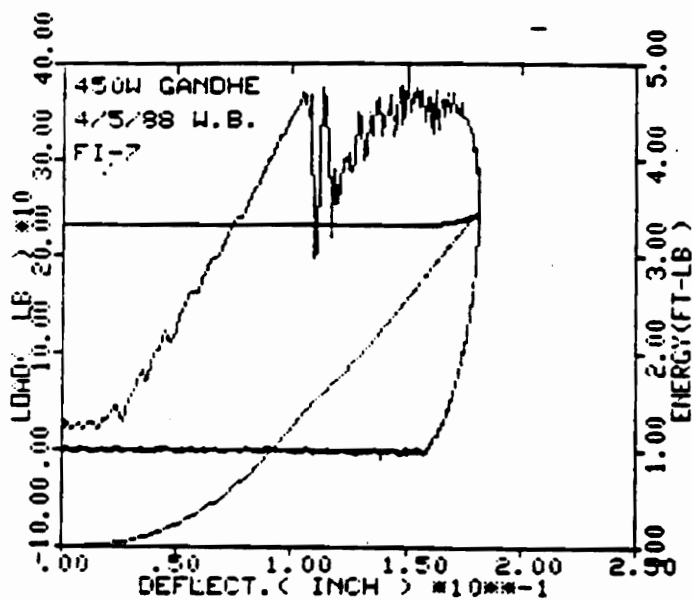


Figure 45. Instrumented impact curves for T300/934 laminate at 3.36 ft-lb.

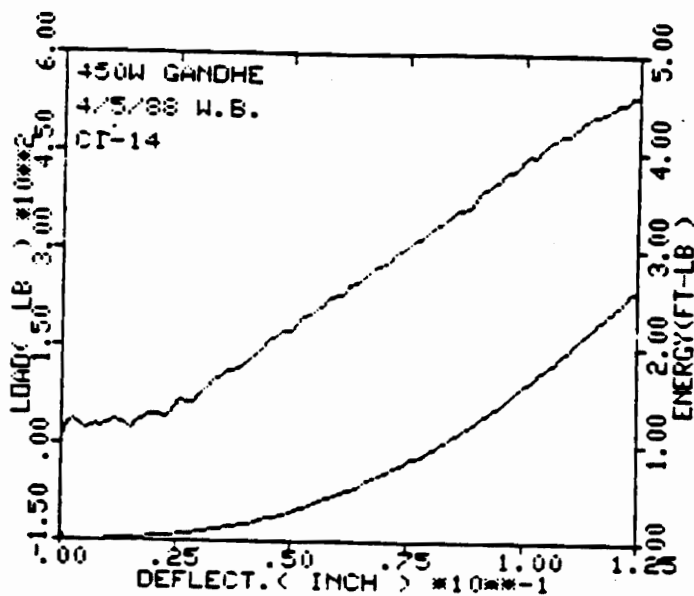


Figure 46. Instrumented impact curves for IM6/1808 laminate at 3.38 ft-lb.

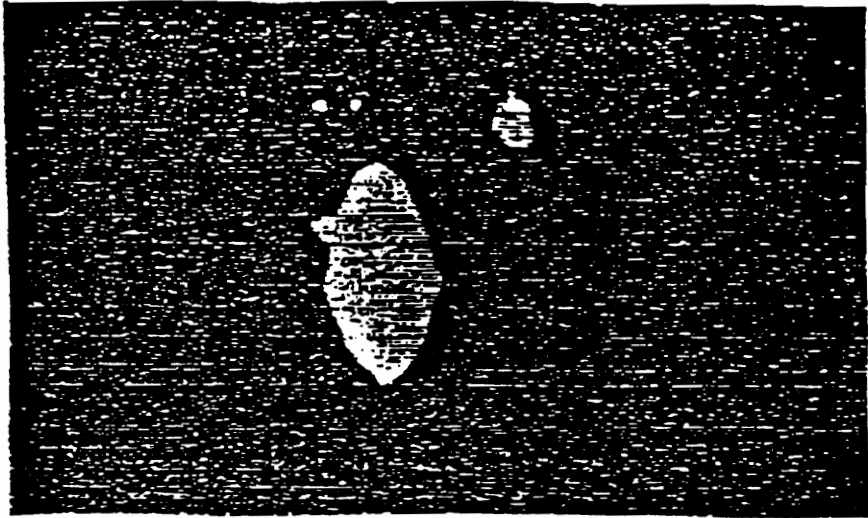


Figure 47. Ultrasonic C-scan image for T300/934 laminate at 3.36 ft-lb.

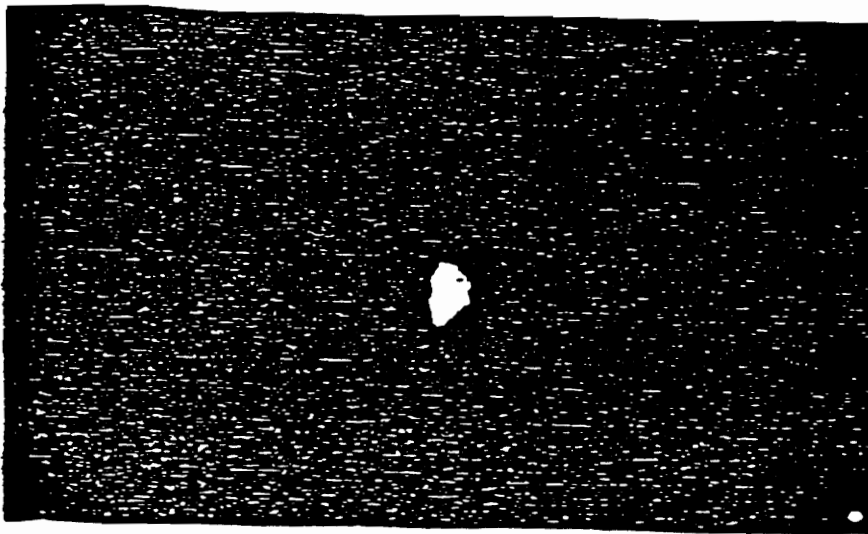


Figure 48. Ultrasonic C-scan image for IM6/1808 laminate at 3.38 ft-lb.

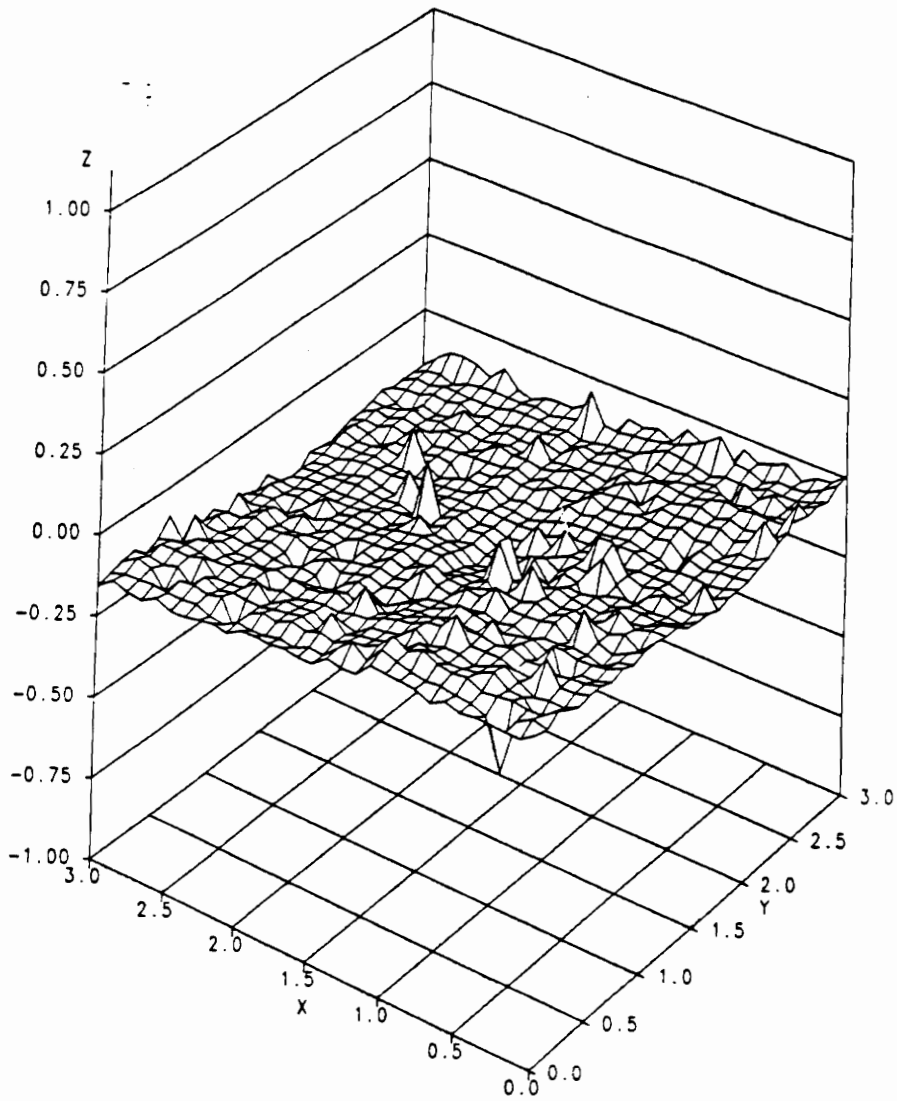


Figure 49. Eddy current 3-D scan for T300/934 laminate at 3.36 ft-lb.

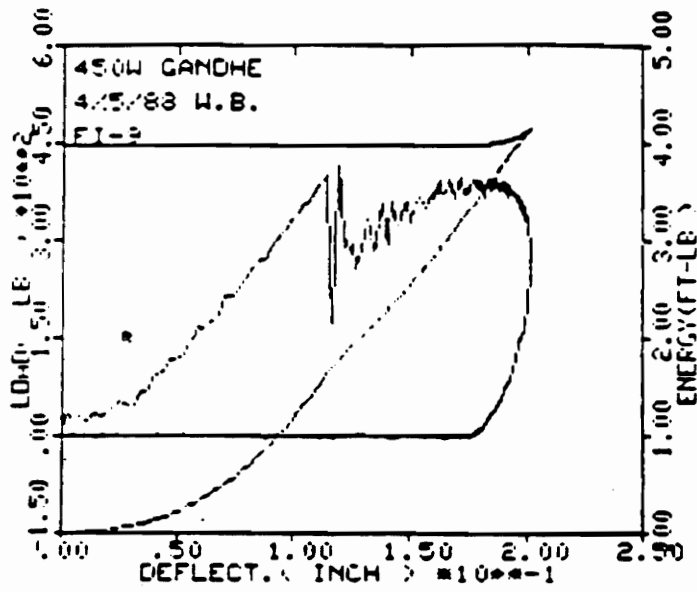


Figure 50. Instrumented impact curves for T300/934 laminate at 4.01 ft-lb.

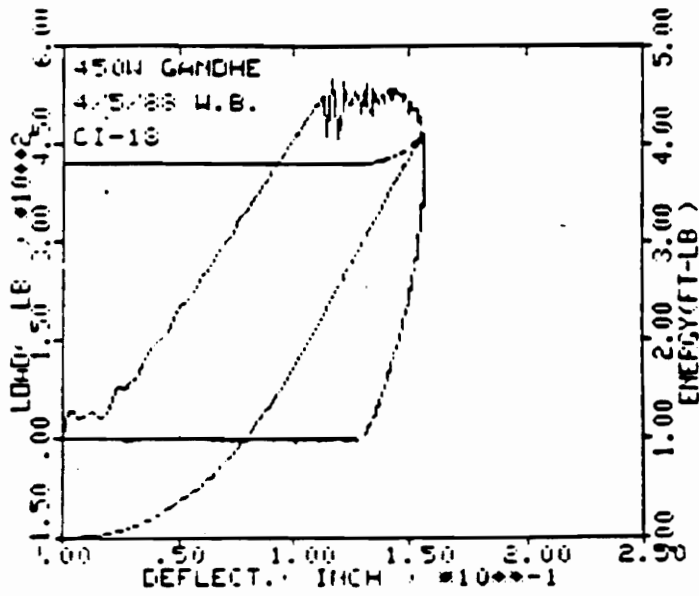


Figure 51. Instrumented impact curves for IM6/1808 laminate at 4.01 ft-lb.

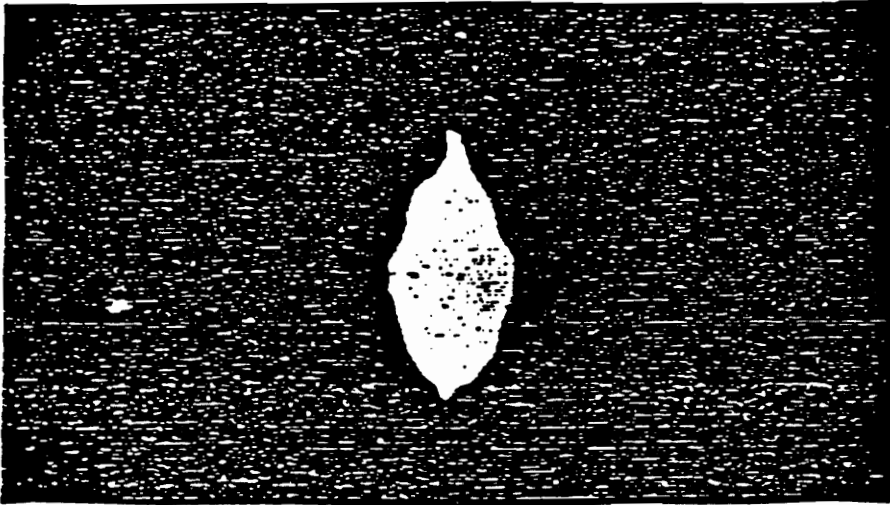


Figure 52. Ultrasonic C-scan image for T300/934 laminate at 4.01 ft-lb.

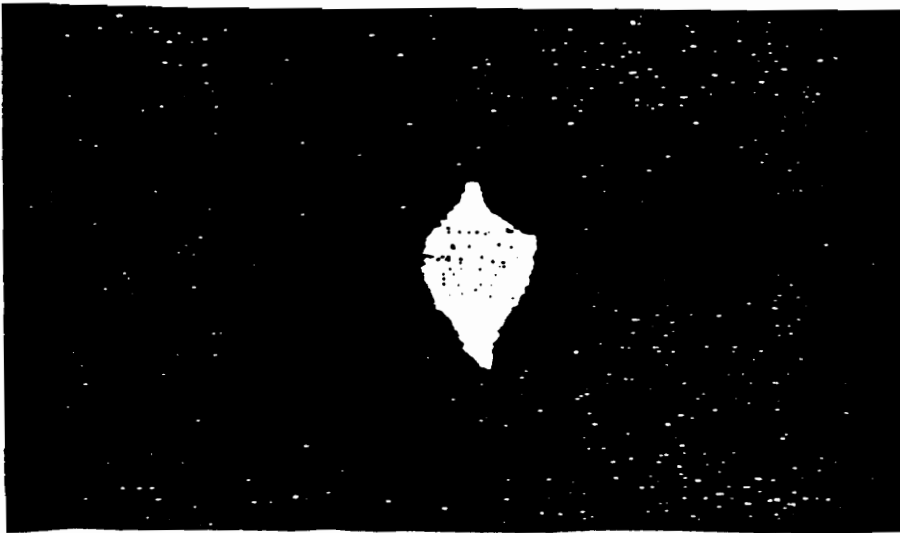


Figure 53. Ultrasonic C-scan image for IM6/1808 laminate at 4.01 ft-lb.

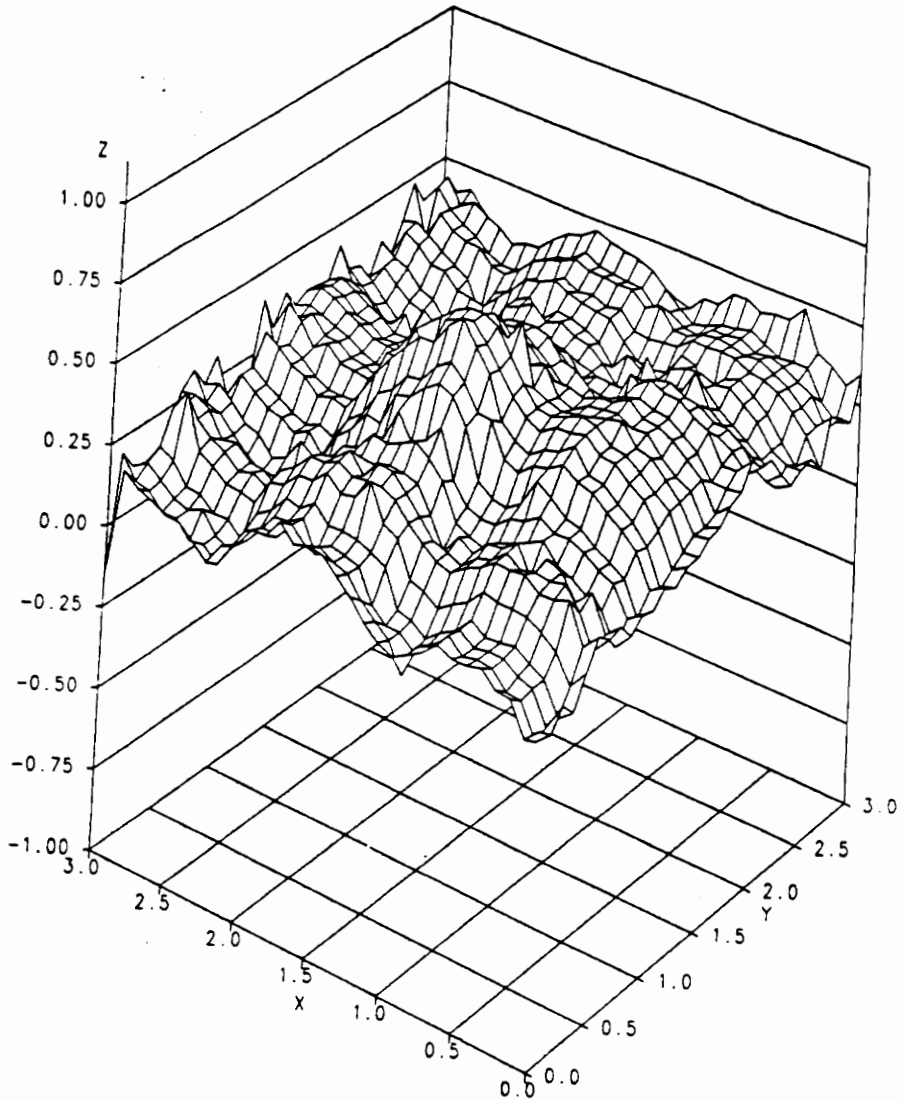


Figure 54. Eddy current 3-D scan for T300/934 laminate at 4.01 ft-lb.

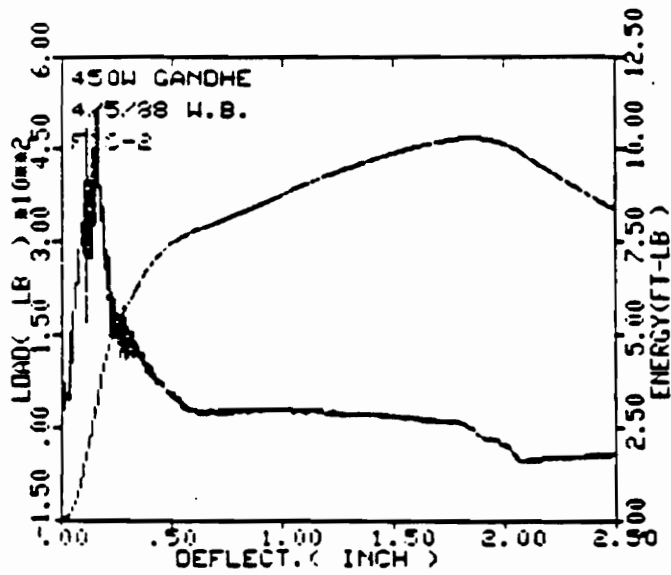


Figure 55. Instrumented Impact plot for through penetration of T300/934 laminate at 10.34 ft-lb.

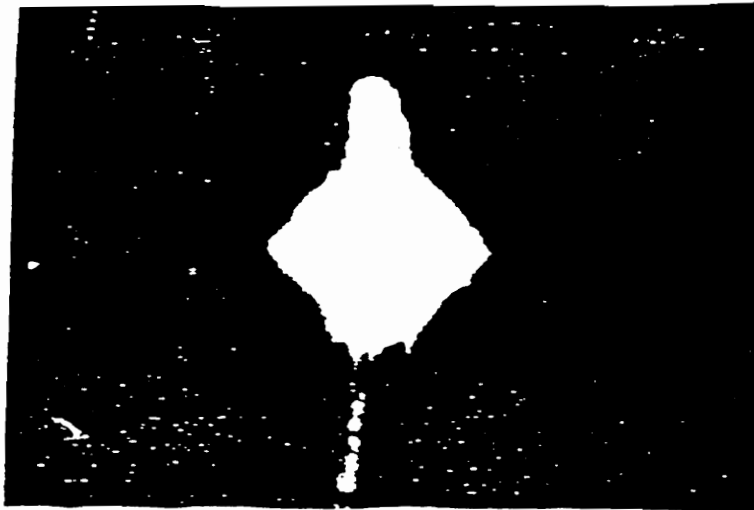


Figure 56. Ultrasonic C-scan image for T300/934 laminate at through penetration impact of 10.34 ft-lb.

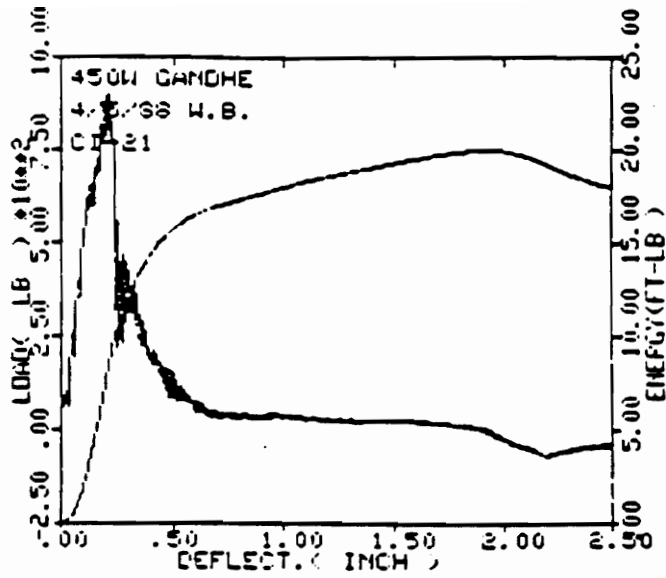


Figure 57. Instrumented Impact plot for through penetration of IM6/1808 laminate at 20.04 ft-lb.

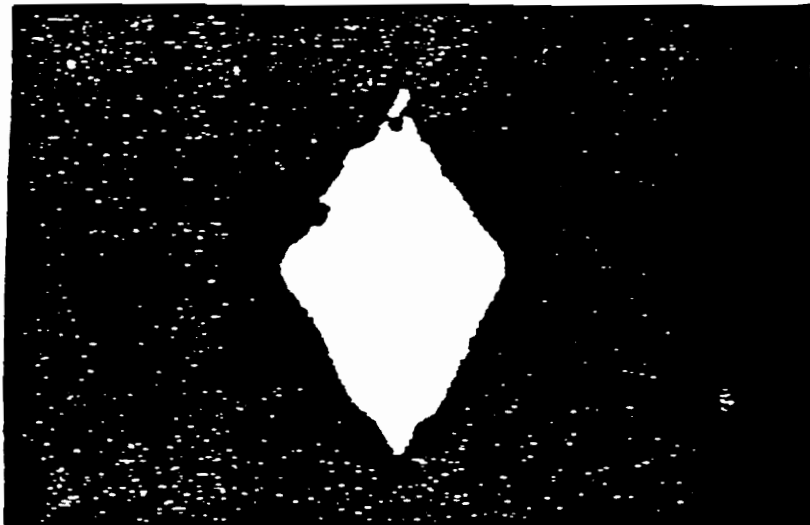


Figure 58. Ultrasonic C-scan image for IM6/1808 laminate at through penetration impact of 20.04 ft-lb.

10.0 VITA

Gajanan Gandhe was born in Bombay, India on March 1st 1964. Gajanan completed his B.S at the Indian Institute of Technology, Bombay in Civil Engineering. Having worked with composite materials in his senior project, Gajanan developed an interest for this field and this brought him to Virginia Tech for his M.S degree. Gajanan has tried to effectively combine his academic background with industrial training on applications of composite materials. His main interests include characterizing new composite materials, industrial applications, and design of composite materials. His hobbies include hiking, traveling, and languages. Gajanan is currently working with the DuPont company at their Chestnut Run plant in Wilmington, Delaware.